



Exploring dynamics of predator-prey interactions: fear, toxicity, carry over and environmental fluctuations

Bijoy Kumar Das^a, Nirapada Santra^a, Guruprasad Samanta^{a,*}

^aDepartment of Mathematics, Indian Institute of Engineering Science and Technology, Shibpur, Howrah - 711103, India

Abstract. Predator-prey has a long background in the ecological environment. The activity of prey's daily life can be altered due to the presence of a predator. Also, some experimental studies have proved that the induced fear of predators felt by prey, has the capability to change both the birth and death rate of the prey species. The effect of such fear and its carry-over impact in a predator-prey model where predators get additional food has been analyzed in a toxic environment. This research delves into the complex dynamics of a predator-prey system within ecological contexts, highlighting the interactions between species and environmental effects. Key factors that are explored include fear effect, additional food for predators, and carry-over effects within a toxic environment. Additionally, the inclusion of a time delay factor accounts for gestation periods, further enriching the dynamic of the system. Environmental fluctuations are studied by incorporating Gaussian white noise into the system, allowing for an analysis of their impact. The study investigates how fear, carry-over effects, and environmental toxicity influence population dynamics. Notably, the delay parameter introduces a supercritical Hopf bifurcation, significantly enhancing the dynamics of the system. Moreover, environmental stochasticity adds complexity to such models by capturing fluctuations in population dynamics. Through bifurcation diagrams, valuable insights are gained about the behavior of the proposed system across various parameter values. This deeper understanding sheds light on the system's stability and response to various environmental influences.

1. Introduction

In the fields of population biology, mathematical biology, and ecology, the predator-prey model has been extensively investigated and used. It gives researchers vision to investigate the complicated relationships between different species and aids in their understanding of the variables affecting population dynamics. Additional aspects including environmental fluctuations, regional concerns and more intricate community structures have been incorporated and modified within the model.

In "An Essay on the Principle of Population", published in 1798, Thomas Robert Malthus examined the relationship between population growth and available resources [1]. As per his opinion, population growth tends to be exponential, or it may tend to rise over a period of time, at a steady percentage rate. He thought that although there was potential for a rapid increase in population, the growth of resources,

2020 *Mathematics Subject Classification.* Primary 92B05; Secondary 92D25, 92D40.

Keywords. Predator-prey interactions; Carry-over effects; Fear effect; Toxicity; Stochastic system.

Received: 10 April 2024; Accepted: 13 April 2024

Communicated by Maria Alessandra Ragusa

* Corresponding author: Guruprasad Samanta

Email addresses: bijoykumardas15@gmail.com (Bijoy Kumar Das), npsantra@gmail.com (Nirapada Santra), g_p_samanta@yahoo.co.uk, gpsamanta@math.iiests.ac.in (Guruprasad Samanta)

especially food, would only be arithmetical or linear. Malthus predicted that this underlying disparity in growth rates would cause the population to eventually outgrow the resources at hand, leading to what he called a “Malthusian crisis.”

The Malthus exponential growth model was altered in the 19th century by Belgian mathematician Pierre François Verhulst, who included the concept of carrying capacity to reflect the larger population sizes that an ecosystem can support [2]. It is also known as logistic growth model. The logistic growth model takes environmental constraints into consideration, in contrast to the Malthusian model, which postulates infinite exponential development. In ecology and population biology, such type of logistic model is applied more broadly to describe population dynamics in situations when resources are limited. It provides a more realistic picture of how populations disperse and endure throughout the entire time period in terms of environmental constraints.

Therefore, in order to construct a predator-prey relationship based on Malthus growth rate, the traditional Lotka-Volterra model was introduced [3, 4]. Differential equations that explain the dynamics of predator and prey populations are the foundation of the Lotka-Volterra model. The model has been further expanded and altered by researchers throughout time in order to take into consideration ecological scenarios that are more plausible. Despite its shortcomings and the fact that real ecosystems are frequently more complicated than the model predicts, the Lotka-Volterra model is nevertheless a key idea in ecological modeling. It has opened the door for the creation of more complex models that seek to depict the complexities of ecological systems. Predator-prey interactions are still a crucial area of study in ecology, because they help us in better understanding of ecosystem dynamics and biodiversity. Researchers have been constructing numerous models to examine the behaviors of this type of ecological models and many other ecological scenarios for so many years [5–11].

Following that, it was changed and evolved into a predator-prey system by adding a predation term—also referred to as a functional response—and a logistic growth term for the prey species. From an ecological perspective, “functional response” refers to a connection involving the size of a prey population and the pace at which a predator consumes its prey. It illustrates how the presence of prey instigates a consumer to change its feeding pace. Mainly three types of functional response are used, namely, Type I Functional Response, Type II Functional Response and Type III Functional Response [12]. There are also some other types of functional responses such as Beddington–DeAngelis, Crowley-Martin, Ratio-dependent functional response, etc. Recognising predator-prey relationships and population dynamics in ecosystems depends significantly on functional responses. By modelling and forecasting the effects of predators on prey populations and vice versa, ecologists and researchers are able to shape the general stability and framework of ecological communities.

Direct and indirect impacts are the two ways in which predators affect prey species. The way that ecological relationships and ecosystem structure are shaped is greatly influenced by these factors. According to several researchers, indirect or non-fatal impacts are even more effective than direct or lethal impacts in creating an unpleasant environment for the prey species.

In many different types of ecosystems, fear is such a non-lethal impact that has a big impact on prey populations [5–7]. The reaction of fear felt by the prey species is frequently an adaptive characteristic that aids in their survival while predators are nearby. There are a few ways how fear may affect the prey species: (i) When the prey species realizes the presence of predators, they frequently display behavioral changes. This may involve adjustments in prey’s diet, mode of mobility, and reproductive strategy. Prey may, for instance, lessen their pursuit levels, become more watchful, or stay away from specific regions where they suspect there is a greater chance of being caught by predator. (ii) Prey populations may have lower rates of successful reproduction as a result of predator fear. Anxiety that arises due to fear can alter the release of hormones that control reproduction, leading to changes in breeding habits and lowering the fertility rates. Regarding population increase, this may also have long-term effects. (iii) The grazing behaviour of prey animals may be altered by induced fear. In situations where they believe that they are in danger due to predators, prey may spend less time grazing. For this, prey species lessen their interaction to other species in the ecosystem. (iv) Prey species can go through evolutionary changes throughout time as a result of their fear of predators. Selected genes can favour characteristics like improved escape methods, heightened awareness, or altered reproductive practices that improve longevity in the face of predators. Sheriff et

al. [13] carried out an experiment on female snowshoe hares (*Lepus Americanus*) in 2009. In the year 2011, Zanette et al. [14] were able to show predators' killing and eating practices have a direct effect on the number of prey. However, the fear of being a victim itself may have a big effect on their behavior, such as making individuals more cautious or less willing to be in the open. A situation involving a tiny colony of song sparrows was portrayed, in which all potential threats to the birds were eliminated. Consequently, it was noted that 40% of the infants were successfully maintained. Predator noises were introduced to numerous pair of birds who were mating; the birds that got used to greater amounts of perceived predator presence selected more isolated nest locations and made fewer grazing visits, both of which were detrimental to the young. The results of these experiments encourage researchers to incorporate fear effects into the prey population in order to enhance the dynamics of the predator-prey model [15–18, 24].

It is necessary to learn about carryover effects in order to fully investigate the ecological dynamics between predators and prey. It emphasizes on how crucial it is to take into account not just direct contacts but also the long-term effects that prior encounters may have on specific prey as well as on the entire populations. In the fields of evolutionary biology and ecology, where scientists seek to gain insight into the intricate interactions between different species within ecosystems, this idea is significantly crucial. Predation events in the past might cause prey animals to change their behavior. The term "carry-over effect" originated from repeated appraisals of clinical testing. In 2014, O'Connor et al. [19] provided the following definition of "carry-over" :

"In an ecological context, carry-over effects can occur in any situation in which an individual's previous history and experience explains their current performance in a given situation".

The authors of this paper propose that ecological carryover effects can also happen across developmental phases, life-history phases, physiological conditions, or social contexts, and that each will have a discrete time-scale. A model with a Holling type II functional response and prey refuge was explored by Mondal and Samanta [20]. Because of the impact of a changing environment, they have also compared their model to a stochastic variant that included Gaussian white noise components. Also Das et al. [21] studied the effect of predator-induced fear and its carry-over impact on a predator-prey model in which the predator species can get some alternative or additional food sources.

Both humans and predator-prey species may be affected in different ways by the presence of toxic materials in their surroundings. The type of toxic substance, how much of it is present, how long the exposure lasts, and the particular biological and ecological traits of the creatures involved, all have an effect on the outcome. Toxic components can cause nausea and respiratory problems, chronic health problems, neurological disorders, cancer, and reproductive problems in human beings. Toxic materials can be introduced to humans through a variety of channels, such as the air, water, soil and food. Mining, inappropriate disposal of waste and industrial operations can all lead to environmental pollution. Also, environmental toxins can have a direct or indirect impact on both predator and prey species. This may cause them to suffer acute consequences that impact their psychological behavior, health, and ability to procreate [22–24].

Time delay is a useful tool in predator-prey models to represent the reality that one population's response to changes in the other population takes time to manifest. Time delays have a big effect on the system's dynamics and can cause fascinating behaviours like oscillations and instability to appear [25–27].

Modifications or shifts in the environment throughout time are referred to as environmental fluctuations. There are two types of fluctuations: long-term ones like those brought on by climate change, and short-term ones like daily or seasonal variations. These changes may have an effect on dynamic populations, ecosystems and the stability of the environment as a whole [28–30]. Variations in the environment can have a major effect on predator-prey systems in a number of ways: (a) Population Dynamics, (b) Behavioral Changes, (c) Resource Availability, (d) Predator-Prey Interactions, etc. All things considered, together with environmental variations are extremely important in determining how predator-prey systems behave.

We summarize this work section-wise in the following way: The foundation of the model has developed in Section 2. In the next Section 3, both the study of positivity and boundedness of our proposed system have been discussed. Thereafter, the evaluation of steady states under some parametric conditions has been shown in the Section 4. The stability analysis of the system has been depicted in Sub-Section 4.1, where

various types of phenomena of the system have been shown. The local bifurcation analysis is studied in Section 5. The inspection with time-delay has been done in Section 6. Next in Section 7, the system has been examined with environmental stochasticity. A brief discussion has been discussed in Section 8.

2. Model Formulation

Let us begin by assuming that, in the absence of predator, the growth rate of the prey species (x_1) follows the logistic law which is given by the following equation:

$$\frac{dx_1}{dt} = \alpha x_1 - m_1 x_1 - d_1 x_1^2, \quad (1)$$

where, α, m_1, d_1 respectively represents the reproductive rate, natural death rate and decay rate due to intraspecific competition. After that, prey biomass is considered with a constant predator biomass (x_2). Numerous studies suggest that the presence of a predator may subsequently affect a prey species' capacity to procreate by creating a fear of the predator that leads to the development of complicated dynamics between them. In contrast to the idea of ingesting a predator directly, we modify the previously discussed logistic growth model to take into consideration induced fear and its effect of carry-over in reproduction of prey, which is represented as follows:

$$\frac{dx_1}{dt} = \alpha x_1 \left(\frac{1 + \beta x_1}{1 + \beta x_1 + \delta x_2} \right) - m_1 x_1 - d_1 x_1^2, \quad (2)$$

here, β denotes the carry-over impact of the predator's instillation of fear, and δ represents that fear. The term $\frac{1 + \beta x_1}{1 + \beta x_1 + \delta x_2}$, say $\zeta(x_1, x_2, \beta, \delta)$, is associated with fear and carry-over effect. This term carry some fascinating information which support biological beliefs too, which are defined as given below:

- (i) The model reduces to a simple prey biomass model with induced fear effect, for $\beta = 0$, as $\zeta(x_1, x_2, 0, \delta) = \frac{1}{1 + \delta x_2}$.
- (ii) For fear level (δ) = 0, the model turns into a simple logistic growth model, which has been already mentioned earlier.
- (iii) Now in absence of predator, i.e., $x_2 = 0$, the prey biomass again follows the logistic growth law, as prey don't have to suffer any danger due to the presence of predator.
- (iv) A larger value of fear is shown to have a detrimental effect on prey biomass. Furthermore, this negative effect can worsen to the point where it affects the prey population's ability to reproduce.
- (v) In a similar manner, one can say that for higher values of x_2 , i.e., predator biomass adversely affect the growth rate of prey biomass.
- (vi) If one increases the value of the parameter β , it brings out a positive impact on the escalation of prey biomass as the prey species learn and gain experience from earlier incidents.
- (vii) Also increasing the number of prey biomass helps them to create a larger community and due to this anti-predator behavior, the reproduction rate of prey species also increases.

The majority of the previous articles dealt with specialized predators, whose development is solely dependent on a particular prey. Predator species may go extinct as a result. It is quite uncommon in ecology to see such kind of predator-prey relationship. When their main food supply is gone, the majority of predators rely on supplementary or alternative food sources in order to stay alive and prevent extinction. In the realm of biological control, it is also one of the well recognized tactics. Therefore, it makes sense to take into account the extra food of constant biomass A that is supplied to the predator species and distributed impartially across the environment. Next, as predator species have more food, the Holling type

II functional response is modified. The calculation of such type of functional response is shown in the previous work [21] and the model takes the following form:

$$\frac{dx_1}{dt} = \alpha x_1 \left(\frac{1 + \beta x_1}{1 + \beta x_1 + \delta x_2} \right) - m_1 x_1 - d_1 x_1^2 - \frac{d_2 x_1 x_2}{\rho + \xi \mu A + x_1}, \tag{3}$$

here, d_2 is the coefficient representing the consumption rate of predator species, ρ is the half saturation constant, ξ is the quality of additional food, μ is the coefficient representing effective quantity of additional food, and A is the additional food biomass.

The following equation represents the increase in predator species linked with the changing type II functional response and natural mortality rate:

$$\frac{dx_2}{dt} = \frac{cd_2(x_1 + \mu A)x_2}{\rho + \xi \mu A + x_1} - m_2 x_2, \tag{4}$$

here c ($0 < c < 1$) is the conversion rate of prey biomass to predator biomass and m_2 is the natural death rate of predator biomass. So our model takes the following form:

$$\begin{aligned} \frac{dx_1}{dt} &= \alpha x_1 \left(\frac{1 + \beta x_1}{1 + \beta x_1 + \delta x_2} \right) - m_1 x_1 - d_1 x_1^2 - \frac{d_2 x_1 x_2}{\rho + \xi \mu A + x_1} \\ \frac{dx_2}{dt} &= \frac{cd_2(x_1 + \mu A)x_2}{\rho + \xi \mu A + x_1} - m_2 x_2. \end{aligned} \tag{5}$$

The impact of man-made and natural environmental contaminants on ecosystem health is rising on a worldwide scale. One of the main global sources of pollution is industrial pollutants. Industrial pollutants can arise from the decomposition of solid waste, discharge and seepage of water, and air level emission and deposition. When it comes to poisons, they can also leak into environment via natural processes. So we added toxic coefficients v_1 and v_2 to both prey species and predator species. For that reason, the final model looks like this:

$$\begin{aligned} \frac{dx_1}{dt} &= \alpha x_1 \left(\frac{1 + \beta x_1}{1 + \beta x_1 + \delta x_2} \right) - m_1 x_1 - d_1 x_1^2 - \frac{d_2 x_1 x_2}{\rho + \xi \mu A + x_1} - v_1 x_1^3, \\ \frac{dx_2}{dt} &= \frac{cd_2(x_1 + \mu A)x_2}{\rho + \xi \mu A + x_1} - m_2 x_2 - v_2 x_2^2, \end{aligned} \tag{6}$$

where the initial conditions are as follows:

$$x_1(0) > 0, x_2(0) > 0. \tag{7}$$

The term ' $v_1 x_1^3$ ' with negative sign is added to the prey species as toxic elements such as industrial pollutants directly effects the prey biomass. After ingesting the affected prey species, predator species also become effected, and that's why they get less affected. So we add ' $-v_2 x_2^2$ ' to the growth of predator species. Here, v_1 and v_2 are toxicant coefficients related to prey and predator species respectively. These coefficients are considered to be positive. Here, it should be mentioned that, $\frac{d(v_1 x_1^3)}{dx_1} = 3v_1 x_1^2 > 0$ and $\frac{d^2(v_1 x_1^3)}{dx_1^2} = 6v_1 x_1 > 0$. As prey species consume an increasing amount of contaminated or poisonous food, it may give rise to a situation where the production of the harmful components related to those species grows more quickly.

Table 1: Description and range of system parameters

Parameter	Description	Range
α	Birth rate of prey	0.2 – 6
m_1	Natural mortality rate of prey	0.01 – 1
d_1	Density dependent decay rate of prey	0.001 – 1
δ	Level of fear	0.05 – 10
β	Carry-over effect rate due to fear	0.01 – 10
d_2	Coefficient of consumption rate of predator	0.1 – 3
ρ	Half saturation constant	0.1 – 5
ξ	Quality of additional food	0.01 – 2
μ	Coefficient of effective quantity of additional food	0.01 – 2
A	Additional food	0.1 – 10
c	Conversion coefficient	0.01 – 1
m_2	Death rate of predator	0.01 – 1
v_1	Toxicity coefficient related to prey	0 – 1
v_2	Toxicity coefficient related to predator	0 – 1

3. Positiveness and Boundedness

Theorem 3.1. *Solution of system (6), with initial conditions (7), exists uniquely and is positive for any time $t \geq 0$.*

Proof. It can be easily verified that the right hand side of system (6) are continuous and locally lipschitzian in \mathbb{R}_+^2 . Hence the solution $(x_1(t), x_2(t))$ of the system exists uniquely on $[0, \eta)$ where $0 < \eta \leq \infty$ [31]. Now from system (6) with initial conditions $x_1(0) > 0$ and $x_2(0) > 0$, we have

$$\begin{aligned}
 x_1(t) &= x_1(0) \exp \left[\int_0^t \left\{ \frac{\alpha(1 + \beta x_1(s))}{1 + \beta x_1(s) + \delta x_2(s)} - m_1 - d_1 x_1(s) - \frac{d_2 x_2(s)}{\rho + \xi \mu A + x_1(s)} - v_1 x_1^2(s) \right\} ds \right] > 0, \\
 x_2(t) &= x_2(0) \exp \left[\int_0^t \left\{ \frac{c d_2 (x_1(s) + \mu A)}{\rho + \xi \mu A + x_1(s)} - m_2 - v_2 x_2(s) \right\} ds \right] > 0.
 \end{aligned}
 \tag{8}$$

This proves that the solution of the proposed system remains positive for any time $t \geq 0$. \square

Next, we show the uniform boundedness of the system’s solution under certain parametric constraints.

Theorem 3.2. *Solutions of system (6), initiating in \mathbb{R}_+^2 , are uniformly bounded, provided $\alpha > m_1$ and $(c d_2 \xi + c d_2 - m_2 \xi) > 0$.*

Proof. From the first equation of system (6), we have

$$\begin{aligned}
 \frac{dx_1}{dt} &\leq \alpha x_1 \left(\frac{1 + \beta x_1}{1 + \beta x_1 + \delta x_2} \right) - m_1 x_1 - d_1 x_1^2 \\
 &\leq (\alpha - m_1) x_1 - d_1 x_1^2 \quad \left[\because \frac{1 + \beta x_1}{1 + \beta x_1 + \delta x_2} \leq 1 \right] \\
 &= (\alpha - m_1) x_1 \left[1 - \frac{x_1}{\frac{\alpha - m_1}{d_1}} \right].
 \end{aligned}$$

$$\therefore \limsup_{t \rightarrow \infty} x_1(t) \leq \frac{\alpha - m_1}{d_1}, \quad \text{as } \alpha > m_1.$$

From the second equation of system (6) we have,

$$\begin{aligned} \frac{dx_2}{dt} &= \frac{cd_2(x_1 + \mu A)x_2}{\rho + \xi\mu A + x_1} - m_2x_2 - v_2x_2^2, \\ &\leq cd_2\left(1 + \frac{1}{\xi}\right)x_2 - m_2x_2 - v_2x_2^2, \\ &= \kappa x_2\left(1 - \frac{x_2}{\frac{\kappa}{v_2}}\right), \text{ assuming } \kappa = \frac{1}{\xi}(cd_2\xi + cd_2 - m_2\xi) > 0. \end{aligned}$$

Which implies $\limsup_{t \rightarrow \infty} x_2(t) \leq \frac{\kappa}{v_2}$, where $\kappa = \frac{1}{\xi}(cd_2\xi + cd_2 - m_2\xi) > 0$.

This demonstrates that any solution of system (6) is uniformly bounded provided, $\alpha > m_1$ and $(cd_2\xi + cd_2 - m_2\xi) > 0$. \square

4. Equilibrium Points

Here we derive some parametric conditions under which various types of steady state solutions of system (6) are emerged, and further we also explore the stability conditions around these steady states. Since the conditions $\alpha > m_1$ and $(cd_2\xi + cd_2 - m_2\xi) > 0$ are sufficient for boundedness of the system solutions, we, therefore restrict our analysis under these parametric constraints.

System (6) always possesses three following boundary equilibrium points:

(i) Trivial equilibrium point: $E_0(0, 0)$

(ii) Axial equilibrium point: $E_{a_1}(x_{1a}, 0)$, where $x_{1a} = \frac{-d_1 + \sqrt{d_1^2 + 4v_1(\alpha - m_1)}}{2v_1}$, provided $\alpha > m_1$. But it is biologically intuitive that higher mortality rate is always harmful for any kind of species and drives that species to extinction, so **throughout this manuscript, we assume that $\alpha > m_1$** .

(iii) Another axial equilibrium point: $E_{a_2}(0, x_{2a})$, where $x_{2a} = \frac{1}{v_2}\left[\frac{cd_2\mu A}{\rho + \xi\mu A} - m_2\right]$, provided $\frac{cd_2\mu A}{\rho + \xi\mu A} > m_2$.

The interior equilibrium point $E_c(x_1^*, x_2^*)$ satisfies the two non-trivial prey and predator nullclines together in the interior of the first quadrant:

$$f_1(x_1, x_2) \equiv \alpha\left(\frac{1 + \beta x_1}{1 + \beta x_1 + \delta x_2}\right) - m_1 - d_1x_1 - \frac{d_2x_2}{\rho + \xi\mu A + x_1} - v_1x_1^2 = 0, \tag{9}$$

$$f_2(x_1, x_2) \equiv \frac{cd_2(x_1 + \mu A)}{\rho + \xi\mu A + x_1} - m_2 - v_2x_2 = 0. \tag{10}$$

From equation (10), we get the explicit expression of x_2^* which is given by

$$x_2^* = \frac{Ac\mu d_2 - A\mu\xi m_2 - \rho m_2 + cd_2x_1^* - m_2x_1^*}{v_2(\xi\mu A + \rho + x_1^*)}.$$

For positive x_2^* , the condition $cd_2(\mu A + x_1^*) > m_2(\mu A\xi + \rho + x_1^*)$ must be satisfied.

Now by using the value of x_2^* in (9), we derive the following equation in x_1 , say $g(x_1) = 0$, where

$$g(x_1) \equiv A_1x_1^6 + A_2x_1^5 + A_3x_1^4 + A_4x_1^3 + A_5x_1^2 + A_6x_1 + A_7 \tag{11}$$

Here, A_i 's ($i = 1, 2, \dots, 7$) are described in Appendix A.

Table 2: Values of parameters used in numerical simulation

Parameter	α	m_1	d_1	δ	β	d_2	ρ	ξ	μ	A	c	m_2	v_1	v_2	σ_1	σ_2
Value	4.83	0.47	0.22	5.3	2.9	0.454	4.07	0.183	0.62	5.77	0.485	0.07	0.094	0.0465	0.009	0.002

4.1. Stability Analysis

Now we investigate the stability behaviour of the system (6) around these equilibrium states by examining the sign of the eigenvalues of the corresponding Jacobian matrix. The Jacobian matrix $J(x_1, x_2)$ of system (6) is given by

$$J(x_1, x_2) = \begin{pmatrix} \frac{\alpha(1+\delta x_2)(1+2\beta x_1)+\alpha\beta^2 x_1^2}{(1+\beta x_1+\delta x_2)^2} - m_1 - 2d_1 x_1 - \frac{(\rho+\xi\mu A)d_2 x_2}{(\rho+\xi\mu A+x_1)^2} - 3v_1 x_1^2 & -\frac{\delta\alpha x_1(1+\beta x_1)}{(1+\beta x_1+\delta x_2)^2} - \frac{d_2 x_1}{\rho+\xi\mu A+x_1} \\ \frac{cd_2(\rho+(\xi-1)\mu A)x_2}{(\rho+\xi\mu A+x_1)^2} & \frac{cd_2(x_1+\mu A)}{\rho+\xi\mu A+x_1} - m_2 - 2v_2 x_2 \end{pmatrix}. \tag{12}$$

Theorem 4.1. *The trivial equilibrium point E_0 is always unstable.*

Proof. At the trivial equilibrium point $E_0(0, 0)$, the Jacobian matrix reduces to

$$J_0 = \begin{pmatrix} \alpha - m_1 & 0 \\ 0 & \frac{cd_2\mu A}{\rho+\xi\mu A} - m_2 \end{pmatrix}.$$

Since one of the eigenvalue is $(\alpha - m_1) > 0$, $E_0(0, 0)$ is unstable. \square

Theorem 4.2. *The axial equilibrium point $E_{a_1}(x_{1a}, 0)$ is stable if $cd_2(x_{1a} + \mu A) < m_2(\rho + \xi\mu A + x_{1a})$ and unstable if $cd_2(x_{1a} + \mu A) > m_2(\rho + \xi\mu A + x_{1a})$, where $x_{1a} = \frac{-d_1 + \sqrt{d_1^2 + 4v_1(\alpha - m_1)}}{2v_1}$.*

Proof. Now the Jacobian matrix at the predator free equilibrium point $E_{a_1}(x_{1a}, 0)$ is given by \square

$$J(x_{1a}, 0) = \begin{pmatrix} (\alpha - m_1) - 2d_1 x_{1a} - 3v_1 x_{1a}^2 & -\frac{\delta\alpha x_{1a}}{(1+\beta x_{1a})} - \frac{d_2 x_{1a}}{\rho+\xi\mu A+x_{1a}} \\ 0 & \frac{cd_2(x_{1a}+\mu A)}{\rho+\xi\mu A+x_{1a}} - m_2 \end{pmatrix}. \tag{13}$$

Thus the eigenvalues of this matrix are $(\alpha - m_1) - 2d_1 x_{1a} - 3v_1 x_{1a}^2$ and $\frac{cd_2(x_{1a}+\mu A)}{\rho+\xi\mu A+x_{1a}} - m_2$. By putting $x_2 = 0$ in (9), we have

$$\alpha - m_1 - d_1 x_{1a} - v_1 x_{1a}^2 = 0 \implies \alpha - m_1 = d_1 x_{1a} + v_1 x_{1a}^2.$$

Hence, with the help of this, first eigenvalue becomes negative. Therefore, the stability of predator free steady state $E_{a_1}(x_{1a}, 0)$ will depend on the sign of the other eigenvalue, i.e., on $\frac{cd_2(x_{1a}+\mu A)}{\rho+\xi\mu A+x_{1a}} - m_2$. So, the result follows.

Theorem 4.3. *The axial equilibrium point $E_{a_2}(0, x_{2a})$ is stable if $\alpha(\rho + \xi\mu A) < (1 + \delta x_{2a}) [m_1(\rho + \xi\mu A) + d_2 x_{2a}]$ and unstable if $\alpha(\rho + \xi\mu A) > (1 + \delta x_{2a}) [m_1(\rho + \xi\mu A) + d_2 x_{2a}]$, where $x_{2a} = \frac{1}{v_2} \left[\frac{cd_2\mu A}{\rho+\xi\mu A} - m_2 \right]$.*

Proof. The Jacobian matrix at the prey free equilibrium point $E_{a_2}(0, x_{2a})$ is given by

$$J(0, x_{2a}) = \begin{pmatrix} \frac{\alpha}{(1+\delta x_{2a})} - m_1 - \frac{d_2 x_{2a}}{(\rho+\xi\mu A)} & 0 \\ \frac{cd_2(\rho+(\xi-1)\mu A)x_{2a}}{(\rho+\xi\mu A)^2} & -v_2 x_{2a} \end{pmatrix}. \tag{14}$$

Thus the eigenvalues of this matrix are $\frac{\alpha}{(1+\delta x_{2a})} - m_1 - \frac{d_2 x_{2a}}{(\rho+\xi\mu A)}$ and $-v_2 x_{2a}$. Therefore, the stability of the prey free steady state $E_{a_2}(0, x_{2a})$ will depend on the sign of the eigenvalue $\frac{\alpha}{(1+\delta x_{2a})} - m_1 - \frac{d_2 x_{2a}}{(\rho+\xi\mu A)}$. So, the result follows. \square

Theorem 4.4. *The coexistence steady state $E_c(x_1^*, x_2^*)$ will be stable if the conditions in the following proof are satisfied.*

Proof. Now the Jacobian matrix at the interior equilibrium point $E_c(x_1^*, x_2^*)$ is given by

$$J(x_1^*, x_2^*) = \begin{pmatrix} a_{11} & a_{12} \\ a_{21} & a_{22} \end{pmatrix} \tag{15}$$

where,

$$\begin{aligned} a_{11} &= \frac{\alpha(1 + \delta x_2^*)(1 + 2\beta x_1^*) + \alpha\beta^2 x_1^{*2}}{(1 + \beta x_1^* + \delta x_2^*)^2} - m_1 - 2d_1 x_1^* - \frac{(\rho + \xi\mu A)d_2 x_2^*}{(\rho + \xi\mu A + x_1^*)^2} - 3v_1 x_1^{*2}, \\ a_{12} &= -\frac{\delta\alpha x_1^*(1 + \beta x_1^*)}{(1 + \beta x_1^* + \delta x_2^*)^2} - \frac{d_2 x_1^*}{\rho + \xi\mu A + x_1^*}, \\ a_{21} &= \frac{cd_2(\rho + (\xi - 1)\mu A)x_2^*}{(\rho + \xi\mu A + x_1^*)^2}, \\ a_{22} &= \frac{cd_2(x_1^* + \mu A)}{\rho + \xi\mu A + x_1^*} - m_2 - 2v_2 x_2^*. \end{aligned}$$

Thus, interior equilibrium point $E_c(x_1^*, x_2^*)$ will be stable if $(a_{11} + a_{22}) < 0$ and $(a_{11}a_{22} - a_{12}a_{21}) > 0$. \square

5. Local Bifurcation

Here, we have examined whether or not the system changes its stability through local bifurcation.

5.1. Transcritical Bifurcation

Theorem 5.1. When additional food A is to be considered as a bifurcating parameter, system (6) exhibits a transcritical bifurcation around the axial steady state E_{a_1} at the critical value $A_{[TC]} = \frac{1}{\mu} \left[\frac{m_2\rho}{cd_2 - m_2\xi} + \frac{m_2 - cd_2}{cd_2 - m_2\xi} x_{1a} \right]$ with $cd_2 > m_2\xi$.

Proof. To prove this theorem, we use Sotomayor’s Theorem [32]. For the critical value $A_{[TC]}$, the Jacobian matrix at the steady state $E_{a_1}(x_{1a}, 0)$ is as follows:

$$J(E_{a_1}; A = A_{[TC]}) = \begin{pmatrix} (\alpha - m_1) - 2d_1 x_{1a} - 3v_1 x_{1a}^2 & -\frac{\delta\alpha x_{1a}}{(1 + \beta x_{1a})} - \frac{d_2 x_{1a}}{\rho + \xi\mu A + x_{1a}} \\ 0 & 0 \end{pmatrix}. \tag{16}$$

Clearly, 0 is an eigenvalue of this matrix. For this eigenvalue, we get two eigenvectors $P = \begin{pmatrix} p_1 \\ 1 \end{pmatrix}$ and $Q = \begin{pmatrix} 0 \\ 1 \end{pmatrix}$ for the Jacobian matrix $J(E_{a_1}; A = A_{[TC]})$ and $[J(E_{a_1}; A = A_{[TC]})]^t$, where

$$p_1 = -\frac{x_{1a} \left(\frac{\alpha\delta}{1 + \beta x_{1a}} + \frac{d_2}{\rho + \xi\mu A + x_{1a}} \right)}{d_1 x_{1a} + 2v_1 x_{1a}^2}.$$

Taking similar notations from [32], we may write down the transversality conditions for transcritical bifurcation as follow:

$$\begin{aligned} \Delta_1 &= Q^t [F_A(E_{a_1}; A = A_{[TC]})] = 0, \\ \Delta_2 &= Q^t [DF_A(E_{a_1}; A = A_{[TC]})P] = \frac{\mu(cd_2 - m_2\xi)}{\rho + \xi\mu A_{[TC]} + x_{1a}} \neq 0, \\ \Delta_3 &= Q^t [D^2F(E_{a_1}; A = A_{[TC]}) (P, P)] = -2v_2 + \frac{p_1(cd_2 - m_2)}{\rho + \xi\mu A_{[TC]} + x_{1a}} \neq 0. \end{aligned}$$

Here, $F \equiv \begin{pmatrix} f_1 \\ f_2 \end{pmatrix}$, where f_1, f_2 are defined earlier. Hence by the help of Sotomayor’s theorem, we can say system (6) shows a transcritical bifurcation in the circumference of the axial steady state E_{a_1} at the critical value $A_{[TC]} = \frac{1}{\mu} \left[\frac{m_2\rho}{cd_2 - m_2\xi} + \frac{m_2 - cd_2}{cd_2 - m_2\xi} x_{1a} \right]$. \square

Theorem 5.2. System (6) exhibits transcritical bifurcation for the bifurcating parameters m_1, m_2 respectively at the critical values $m_{1T} = \alpha - 2d_1x_{1a} - 3v_1x_{1a}^2$ and $m_{2T} = \frac{cd_2(x_{1a} + \mu A)}{\rho + \xi\mu A + x_{1a}}$, where $x_{1a} = \frac{-d_1 + \sqrt{d_1^2 + 4v_1(\alpha - m_1)}}{2v_1}$ around the axial steady state E_{a_1} .

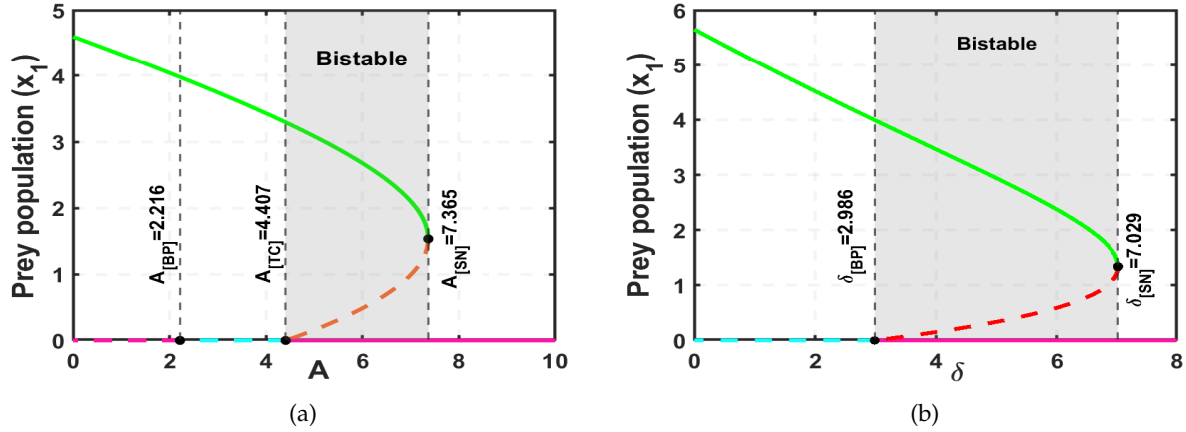


Figure 1: (a) One parameter bifurcation diagram with respect to A . (b) One parameter bifurcation diagram with respect to δ . Solid green curve indicates stable interior equilibrium E_{c_1} , red dotted curve denotes unstable interior equilibrium E_{c_2} , pink solid curve indicates stable E_{a_2} where as dashed cyan color indicates unstable one and dashed pink curve indicates unstable E_0 .

In Figure 1, the bifurcation diagrams with respect to the parameter A and δ have been depicted. From Figure 1a it is clear that at $A_{[BP]} = 2.216$, there is a branch point and branches are unstable E_0 and unstable E_{a_2} . A transcritical and a saddle node bifurcation occurs at $A_{[TC]} = 4.407$ and $A_{[SN]} = 7.365$ respectively. The highlighted region in the figures indicates that the bistability phenomenon occurs between the interior equilibrium points E_c and prey free equilibrium E_{a_2} . Similarly, Figure 1b shows that the system exhibits transcritical and saddle node bifurcation at $\delta_{[TC]} = 2.986$ and $\delta_{[SN]} = 7.029$ respectively.

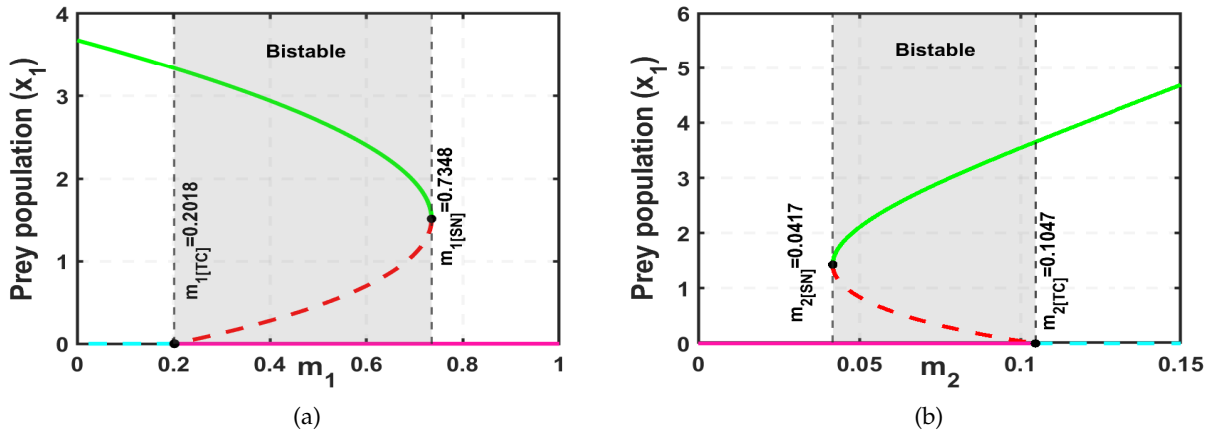


Figure 2: (a) One parameter bifurcation diagram with respect to m_1 (b) one parameter bifurcation diagram with respect to m_2 . Solid green curve indicates stable equilibrium E_{c_1} , red dotted curve denotes unstable E_{c_2} , pink solid curve indicates stable E_{a_2} where as dashed cyan color indicates unstable one.

Figure 2 demonstrates the bifurcation scenarios regarding the parameters m_1 and m_2 . Both the figures

have similar types of phenomena. The proposed system exhibits transcritical as well as saddle node bifurcation for both the parameters at $m_{1[TC]} = 0.2018$, $m_{2[TC]} = 0.1047$ and $m_{1[SN]} = 0.7348$, $m_{2[SN]} = 0.0417$ respectively. Bifurcation diagrams with respect to v_1 , v_2 and β have been depicted in Figure 3. Figure 3a

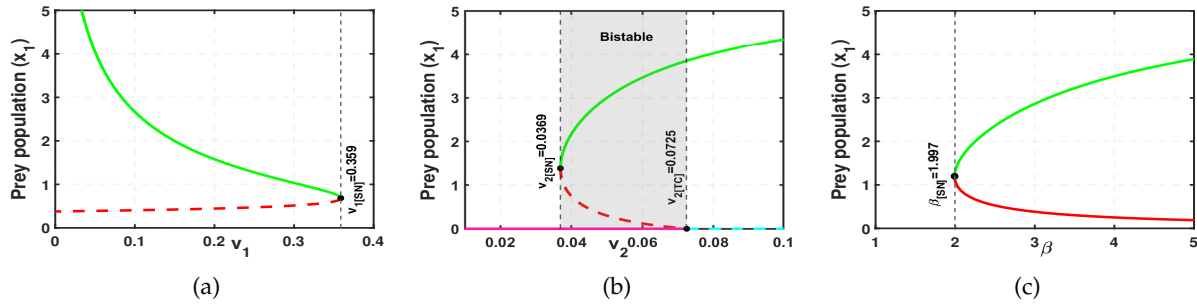


Figure 3: (a) Bifurcation diagram with respect to v_1 (b) bifurcation diagram with respect to v_2 (c) Bifurcation diagram with respect to β . Solid green curve indicates stable equilibrium E_{c_1} , red dotted curve denotes unstable E_{c_2} , pink solid curve indicates stable E_{a_2} where as dashed cyan color indicates unstable one.

indicates that the system exhibits a saddle node bifurcation at $v_{1[SN]} = 0.359$ about the interior equilibrium point. A transcritical and a saddle node bifurcation occur at $v_{2[TC]} = 0.0725$ and at $v_{2[SN]} = 0.0369$ respectively as shown in Figure 3b. Figure 3c demonstrates that the system exhibits saddle node bifurcation about the interior equilibrium point at $\beta_{[SN]} = 1.997$.

In Figure 4, two parametric bifurcation diagrams have been depicted in m_1m_2 and v_1v_2 -plane. In m_1m_2 -plane, the regions divided by the saddle node and transcritical bifurcation curves are defined by B_1 , B_2 , B_3 and B_4 . In the region B_1 the prey free equilibrium E_{a_2} is stable where as coexistence equilibrium is stable in B_3 and predator free is in B_4 . The region B_2 is the bistable region where bistability occurs between E_{a_2} and E_{c_1} . In v_1v_2 -plane, the B_5 is the region where prey free equilibrium E_{a_2} is stable, and B_6 is the bi-stable region where bistability occurs between E_{c_1} and E_{a_1} . In the region B_7 , E_{c_1} is stable. The stability nature of system (6) in various regions of m_1m_2 and v_1v_2 -plane are described in Table 3 in details.

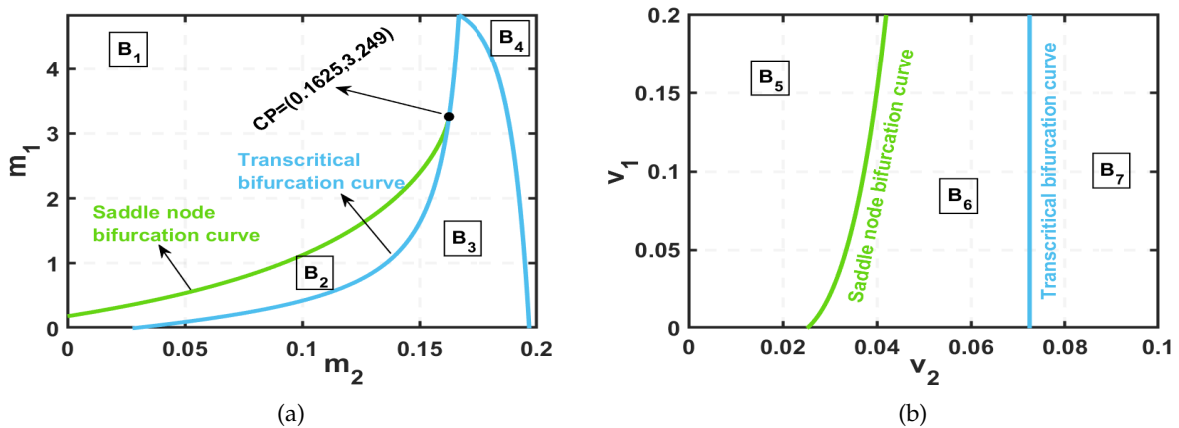


Figure 4: (a) Two parametric bifurcation curves in m_1m_2 -plane (b) Two parametric curves in v_1v_2 -plane.

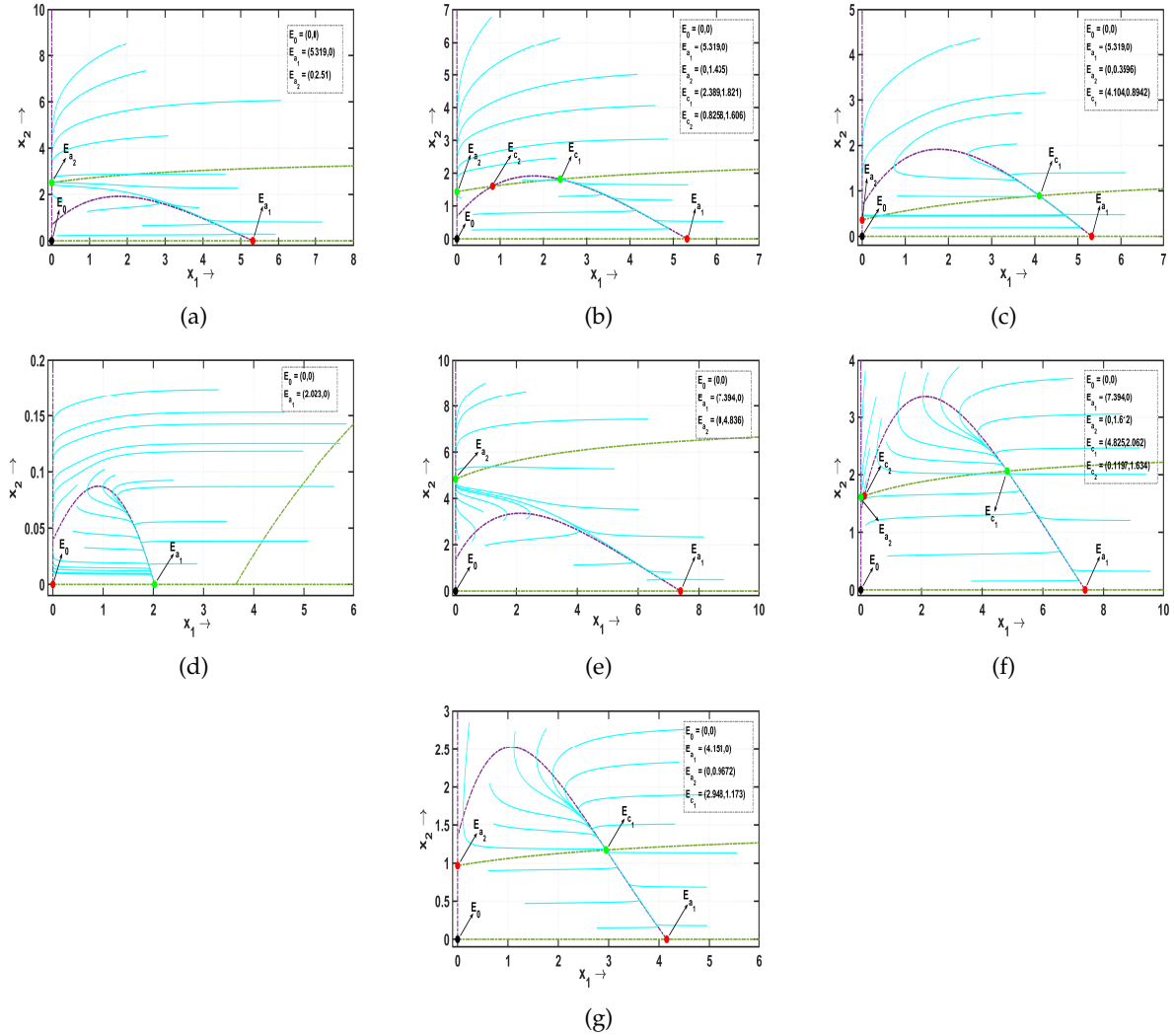


Figure 5: Phase portraits and nullclines taking point from (a) Region B_1 (b) Region B_2 (c) Region B_3 (d) Region B_4 (e) Region B_5 (f) Region B_6 (g) Region B_7 . Here, (●), (●), (●), (---) and (---) denotes unstable node, saddle point, stable node, prey-nullcline and predator-nullcline respectively.

Table 3: Descriptions of stability nature of the system (6) in m_1m_2 and v_1v_2 -plane

Region	Nature of stability					Type of region
	E_0	E_{a_1}	E_{a_2}	E_{c_1}	E_{c_2}	
B_1	unstable node	saddle	stable node			Monostable
B_2	unstable node	saddle	stable node	stable node	saddle	Bistable
B_3	unstable node	saddle	saddle	stable node		Monostable
B_4	saddle	stable node				Monostable
B_5	unstable node	saddle	stable node			Monostable
B_6	unstable node	saddle	stable node	stable node	saddle	Bistable
B_7	unstable node	saddle	saddle	stable node		Monostable

To visually illustrate the dynamic behavior of the system (6) within the specified region outlined in Table 3, we have constructed a detailed depiction showcasing the phase portrait and nullcline, as presented in Figure 5. By varying the initial conditions, we have illustrated the presence of distinct equilibrium points, including stable nodes, unstable nodes, and saddle points. This graphical representation provides valuable insights into the system’s behavior and stability across different starting conditions, enhancing our understanding of its dynamic nature within the defined parameter space.

6. Delayed Model

Broadly speaking, time delay is the amount of time a system takes to react to an input or change. Time delay is commonly expressed by incorporating a delay component into a mathematical model. This idea is especially important in systems where actions have to be delayed, rather than instantaneous, repercussions. Time delays can be expressed as functions or state variables at a former time affecting the system’s current state. For the following reasons, time delays may be taken into account in an ecological model: (i) Gestation and Maturation Time; (ii) Time Lag in Population Response; (iii) Time for Migration or Dispersal; (iv) Environmental Factors; (v) Evolutionary Changes. Predator-prey models can better represent the real-life dynamics and relationships found in ecological systems by incorporating time delays. It makes possible to depict the temporal components of predator-prey relationships more accurately, which improves our comprehension of how populations react to changes over time.

6.1. Stability analysis about the interior equilibrium point

$$\begin{aligned} \frac{dx_1}{dt} &= \alpha x_1 \left(\frac{1 + \beta x_1}{1 + \beta x_1 + \delta x_2} \right) - m_1 x_1 - d_1 x_1^2 - \frac{d_2 x_1 x_2}{\rho + \xi \mu A + x_1} - v_1 x_1^3, \quad x_1(0) > 0 \\ \frac{dx_2}{dt} &= \frac{cd_2(x_1(t - \tau) + \mu A)x_2(t - \tau)}{\rho + \xi \mu A + x_1(t - \tau)} - m_2 x_2 - v_2 x_2^2, \quad x_2(0) > 0 \end{aligned} \tag{17}$$

The initial conditions are taken as:

$x_1(\psi) = u_1(\psi), x_2(\psi) = u_2(\psi), \psi \in [-\tau, 0]$, where the function $u = (u_1, u_2)$ belongs to the Banach space $C = C([-\tau, 0], \mathbb{R}_+^2)$. It is considered that $u_j(0) > 0, j = 1, 2$, biologically which are meaningful.

Let us perform the transformations $x_1 = X_1 + x_1^*$ and $x_2 = X_2 + x_2^*$, so that system (17) be linearized about the coexistence steady state $E_c = (x_1^*, x_2^*)$ as:

$$\frac{dV_1}{dt} = Q_1 V_1(t) + Q_2 V_1(t - \tau). \tag{18}$$

Here, $V_1 = [X_1 \ X_2]^T, Q_1 = \begin{bmatrix} a_{11} & a_{12} \\ 0 & a_{22} \end{bmatrix}$ and $Q_2 = \begin{bmatrix} 0 & 0 \\ c_{21} & c_{22} \end{bmatrix}$, where

$$a_{11} = \frac{\alpha(1 + \delta x_2)(1 + 2\beta x_1) + \alpha\beta^2 x_1^2}{(1 + \beta x_1 + \delta x_2)^2} - m_1 - 2d_1 x_1 - \frac{(\rho + \xi \mu A)d_2 x_2}{(\rho + \xi \mu A + x_1)^2} - 3v_1 x_1^2, \tag{19}$$

$$a_{12} = \frac{\delta \alpha x_1(1 + \beta x_1)}{(1 + \beta x_1 + \delta x_2)^2} - \frac{d_2 x_1}{\rho + \xi \mu A + x_1}, \quad a_{22} = -m_2 - 2v_2 x_2^*, \tag{20}$$

$$c_{21} = \frac{cd_2(\rho + (\xi - 1)\mu A)x_2^*}{(\rho + \xi \mu A + x_1^*)^2}, \quad c_{22} = \frac{cd_2(x_1^* + \mu A)}{\rho + \xi \mu A + x_1^*}. \tag{21}$$

The characteristic equation of (18) can be expressed as follows:

$$\lambda^2 + M_{a1}\lambda + M_{a2} + (N_{a1}\lambda + N_{a2})e^{-\lambda\tau} = 0, \tag{22}$$

where, $M_{a1} = -(a_{11} + a_{22})$, $M_{a2} = a_{11}a_{22}$, $N_{a1} = -c_{22}$ and $N_{a2} = a_{11}c_{22} - a_{12}c_{21}$.

For $\tau \neq 0$, the nature of stability of the coexistence equilibrium E_c depends on the sign of the roots of the characteristic equation (22). The system (18) is locally asymptotically stable if real parts of all the roots of the characteristic equation (22) are negative. For the non-delayed system, we first assume that E_c is asymptotically stable and find the parametric conditions under which E_c is stable, including the delay. It is known that due to the continuity property of the delay parameter τ , the characteristic equation (22) has roots with positive real parts if and only if it has purely imaginary roots. With this information, we can derive the parametric conditions under which equation (22) has only roots with negative real part so that interior steady state E_c becomes locally asymptotically stable. Suppose, $\lambda(\tau) = p_1(\tau) + iq_1(\tau)$ be a root of equation (22). However, since $\tau = 0$ indicates that the coexistence equilibrium point E_c is stable, it follows that $p_1(0) < 0$. It can be demonstrated that $p_1(\tau) < 0$ and the coexistence equilibrium point E_c remain stable for sufficiently smaller values of $\tau > 0$. For the threshold value τ^* (say) of τ , $\lambda(\tau)$ becomes purely imaginary, i.e., $p_1(\tau^*) = 0$ and $q_1(\tau^*) \neq 0$. The instability of E_c occurs when τ reaches the critical value τ^* . In contrast, the steady state E_c will always be stable regardless of any τ if there is no τ^* occurs for which $\lambda(\tau^*)$ is purely imaginary. We examine the real and imaginary parts of the equation (22) by replacing $\lambda = p_1 + iq_1$, and then we set $p_1 = 0$.

Now, we obtain:

$$N_{a2} \cos q_1\tau + N_{a1}q_1 \sin q_1\tau = q_1^2 - M_{a2} \tag{23}$$

$$N_{a1}q_1 \cos q_1\tau - N_{a2} \sin q_1\tau = -M_{a1}q_1 \tag{24}$$

We have, from equations (23) and (24) by eliminating τ ,

$$q_1^4 + (M_{a1}^2 - N_{a1}^2 - 2M_{a2})q_1^2 + M_{a2}^2 - N_{a2}^2 = 0. \tag{25}$$

Putting $q_1^2 = \zeta_1$, we have

$$\Psi(\zeta_1) \equiv \zeta_1^2 + (M_{a1}^2 - N_{a1}^2 - 2M_{a2})\zeta_1 + M_{a2}^2 - N_{a2}^2 = 0 \tag{26}$$

which is a second degree equation in ζ_1 . Since, $\Psi(\infty) = \infty$, so equation (26) has at least one positive real root if $\Psi(0) < 0$, i.e., if $M_{a2}^2 < N_{a2}^2$.

Let, $\zeta_1 = \zeta_1^*$ be a positive root of (26), then $q_1 = \sqrt{\zeta_1^*}$.

In 2003, Ruan and Wei [33] developed a lemma, which is given as:

Lemma 6.1. Consider the exponential polynomial

$$\begin{aligned} P(\lambda, e^{-\lambda\tau_1}, e^{-\lambda\tau_2}, \dots, e^{-\lambda\tau_m}) &= \lambda^n + p_1^{(0)}\lambda^{n-1} + \dots + p_{n-1}^{(0)}\lambda + p_n^{(0)} \\ &+ [p_1^{(1)}\lambda^{n-1} + \dots + p_{n-1}^{(1)}\lambda + p_n^{(1)}]e^{-\lambda\tau_1} \\ &+ [p_1^{(2)}\lambda^{n-1} + \dots + p_{n-1}^{(2)}\lambda + p_n^{(2)}]e^{-\lambda\tau_2} \\ &+ \dots \\ &+ [p_1^{(m)}\lambda^{n-1} + \dots + p_{n-1}^{(m)}\lambda + p_n^{(m)}]e^{-\lambda\tau_m}, \end{aligned}$$

where $\tau_i \geq 0$, ($i = 1, 2, \dots, m$) and $p_j^{(i)}$, ($i = 0, 1, 2, \dots, m; j = 1, 2, \dots, n$) are constants. If $(\tau_1, \tau_2, \dots, \tau_m)$ vary, the sum of the orders of zero of $P(\lambda, e^{-\lambda\tau_1}, e^{-\lambda\tau_2}, \dots, e^{-\lambda\tau_m})$ in the open half plane can change only if a zero appears on or crosses the imaginary axis.

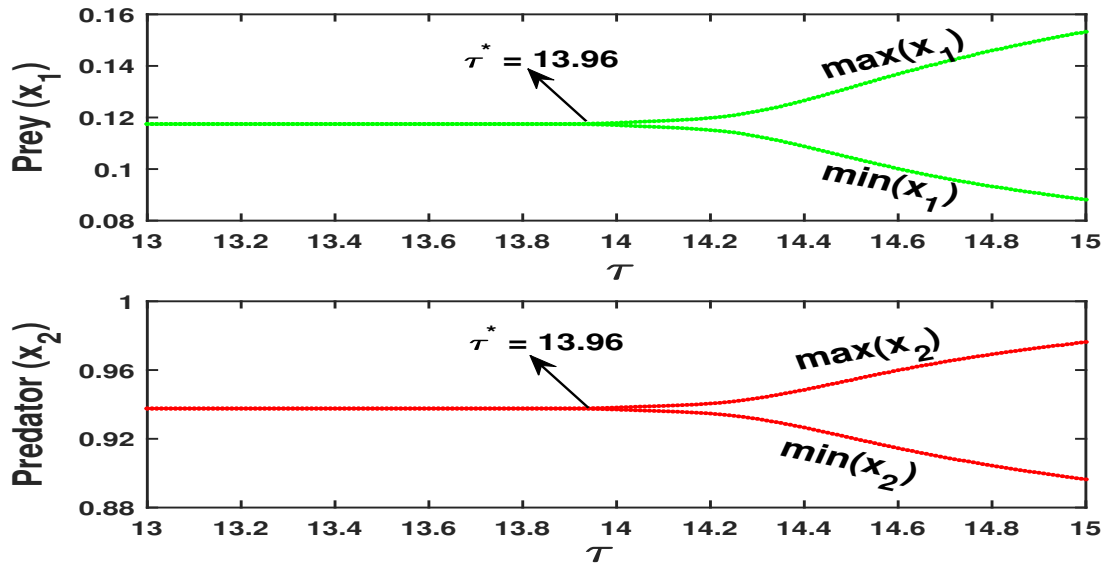


Figure 6: Bifurcation diagram of the prey and predator populations corresponding to delayed system (17). Here, $\alpha = 0.5, \beta = 0.5, \delta = 1, m_1 = 0.1, d_1 = 0.38, d_2 = 0.08, \rho = 0.4, \xi = 0.7, \mu = 0.3, A = 0.5, c = 0.9, m_2 = 0.12, v_1 = 0.002, v_2 = 0.0015$.

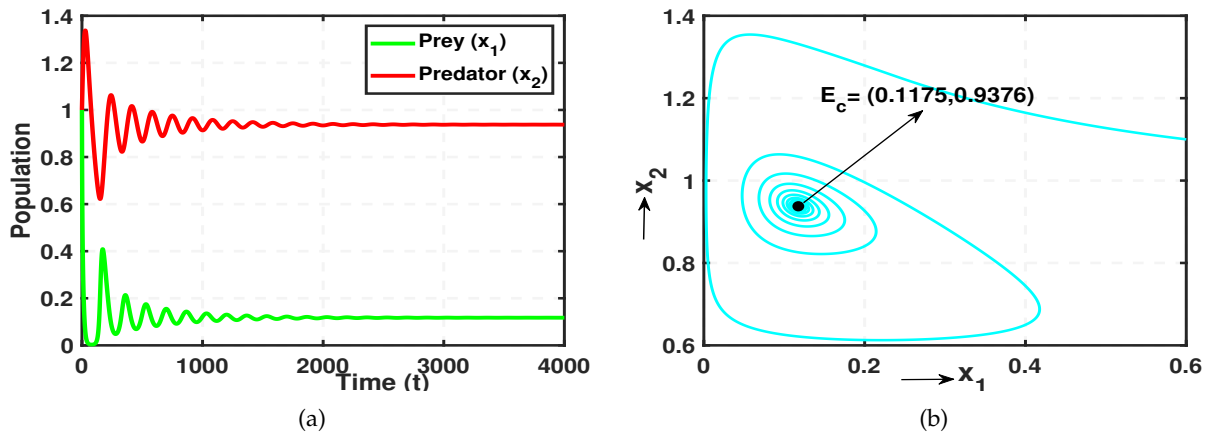


Figure 7: (a) Time series plot of the species corresponding to the delayed system (b) Phase portrait. Here, $\tau = 9 < \tau^*$ and other parameters values are same as in Figure 6.

Theorem 6.2. Let the coexistence steady state E_c is LAS for non-delayed system of (17) (that is at $\tau = 0$). Then delayed system (17) is LAS near E_c with the parametric condition $M_{a2}^2 < N_{a2}^2$, if τ is less than a threshold value τ^* (if exists) of τ and unstable for $\tau > \tau^*$, where

$$\tau_+^{(j)} = \frac{1}{\sqrt{\zeta_1^*}} \cos^{-1} \left\{ \frac{\zeta_1^* (N_{a2} - M_{a1} N_{a1}) - M_{a2} N_{a2}}{N_{a1}^2 \zeta_1^* + N_{a2}^2} \right\} + \frac{2\pi j}{\sqrt{\zeta_1^*}}, \quad j = 0, 1, 2, 3, \dots \tag{27}$$

and $\tau^* = \tau_+^{(0)}$ (minimum value). Consequently, model (17) experiences a Hopf-bifurcation about E_c at $\tau = \tau^*$ provided $A_1 C_1 > B_1 D_1$, where A_1, B_1, C_1 and D_1 are described in the proof.

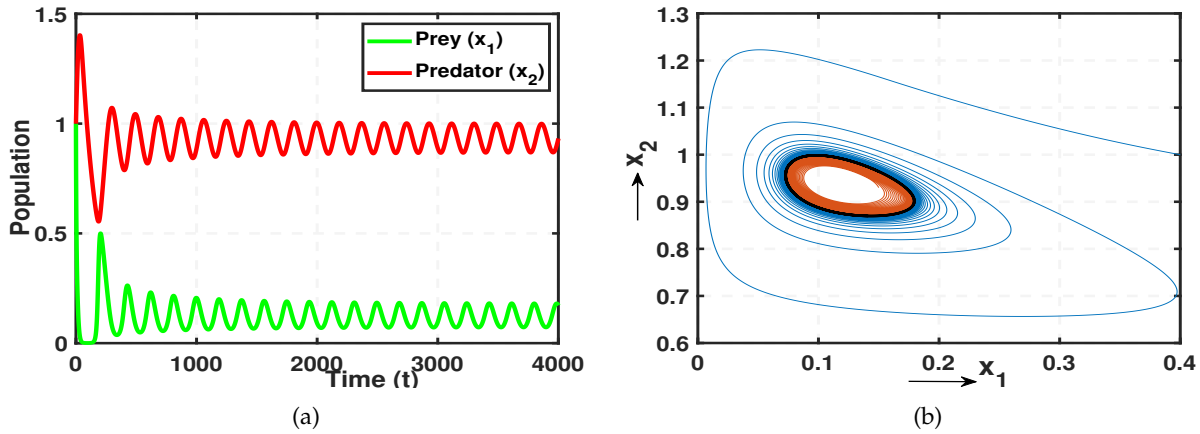


Figure 8: **(a)** Time series plot of the species **(b)** Phase portrait. (—) indicates the stable limit cycle around the unstable equilibrium point. Here, $\tau = 16 > \tau^*$ and other parameters values are same as in Figure 6.

Proof. For $M_{a2}^2 < N_{a2}^2$, a positive root, ζ_1^* , (say) arises from the equation (26). With the help of the equations (23) and (24), a function $\tau_+^{(j)}$ (say) of ζ_1^* is obtained, where $j = 0, 1, 2, 3, \dots$; which can be written as:

$$\tau_+^{(j)} = \frac{1}{\sqrt{\zeta_1^*}} \cos^{-1} \left\{ \frac{\zeta_1^*(N_{a2} - M_{a1}N_{a1}) - M_{a2}N_{a2}}{N_{a1}^2\zeta_1^* + N_{a2}^2} \right\} + \frac{2\pi j}{\sqrt{\zeta_1^*}}, \quad j = 0, 1, 2, 3, \dots$$

Therefore, for delayed system (17) with $\tau < \tau^*$, the interior equilibrium point E_c will remain stable. The next step is to determine whether or not the transversality criterion $\left[\frac{d}{d\tau} Re(\lambda(\tau)) \right]_{\tau=\tau^*} > 0$ is met. We use $\lambda = p_1 + iq_1$ and plug it into equation (22) to investigate the transversality criteria. Following a separation of real and imaginary components and the differentiation with respect to τ , and after setting $p_1 = 0$ and $\tau = \tau^*$, we get:

$$A_1 \left[\frac{d}{d\tau} Re(\lambda(\tau)) \right]_{\tau=\tau^*} + B_1 \left[\frac{d}{d\tau} Im(\lambda(\tau)) \right]_{\tau=\tau^*} = C_1, \tag{28}$$

$$-B_1 \left[\frac{d}{d\tau} Re(\lambda(\tau)) \right]_{\tau=\tau^*} + A_1 \left[\frac{d}{d\tau} Im(\lambda(\tau)) \right]_{\tau=\tau^*} = D_1, \tag{29}$$

where,

$$A_1 = \left[M_{a1} + N_{a1} \cos(q_1\tau) - N_{a2}\tau \cos(q_1\tau) - N_{a1}q_1\tau \sin(q_1\tau) \right]_{\tau=\tau^*, q_1=\sqrt{\zeta_1^*}}$$

$$B_1 = \left[-2q_1 + N_{a1} \sin(q_1\tau) - N_{a2}\tau \sin(q_1\tau) + N_{a1}q_1\tau \cos(q_1\tau) \right]_{\tau=\tau^*, q_1=\sqrt{\zeta_1^*}}$$

$$C_1 = \left[N_{a2}q_1 \sin(q_1\tau) - N_{a1}q_1^2 \cos(q_1\tau) \right]_{\tau=\tau^*, q_1=\sqrt{\zeta_1^*}}$$

$$D_1 = \left[N_{a2}q_1 \cos(q_1\tau) + N_{a1}q_1^2 \sin(q_1\tau) \right]_{\tau=\tau^*, q_1=\sqrt{\zeta_1^*}}$$

Solving equations (28) and (29), we obtain:

$$\left[\frac{d}{d\tau} Re(\lambda(\tau)) \right]_{\tau=\tau^*} = \frac{A_1C_1 - B_1D_1}{A_1^2 + B_1^2}.$$

For $B_1D_1 < A_1C_1$, $\left[\frac{d}{d\tau} Re(\lambda(\tau)) \right]_{\tau=\tau^*} > 0$. Hence, the transversality condition is verified. \square

The bifurcation diagram which is depicted in Figure 6 illustrates the behavior of the delayed system (17). Notably, the diagram reveals a significant occurrence known as a Hopf bifurcation, manifesting precisely at the critical point $\tau^* = 13.96$. This pivotal point marks a transition in the system’s stability characteristics. Specifically, for delay parameter values τ less than the critical value 13.96, the system exhibits stability, while for values exceeding τ^* , the system becomes unstable. To gain a more intuitive understanding of this phenomenon, we have conducted a comparative analysis using two distinct values of τ : $\tau = 9 < \tau^*$ and $\tau = 16 > \tau^*$. The resulting time series and phase portraits are presented in Figure 7 and Figure 8 respectively. Figure 7 portrays the behavior of the system for $\tau = 9$, showcasing a stable nature. The phase portrait, denoted by the cyan solid line, converges towards the state $E_c(0.1175, 0.9376)$. This indicates that trajectories in the phase space tend towards this stable equilibrium point over time. In contrast, Figure 8 illustrates the dynamics of the system corresponding to $\tau = 16$. Notably, for this value of τ , the system exhibits oscillatory behavior. The phase portrait demonstrates trajectories converging towards a stable limit cycle, indicated by the black colored closed curve. Thus, the analysis elucidates the important role of the delay parameter τ in determining the stability and dynamical behavior of the system.

7. Study of System (6) with Environmental Stochasticity

Assume that the environmental fluctuations will manifest themselves primarily as fluctuations in the natural mortality rate of each species, since these are the main parameters subject to coupling of a prey–predator pair with its environment. These parameters are perturbed by Gaussian white noise, which is one of the most useful noises for modeling rapidly fluctuating phenomena.

Thus, we use Gaussian white noises γ_1 and γ_2 in system (6) to perturb the parameters m_1 and m_2 . Here, γ_1 and γ_2 are independent Gaussian white noises having the following properties:

$$\langle \gamma_i(t) \rangle = 0 \text{ and } \langle \gamma_i(t_1)\gamma_i(t_2) \rangle = \mu_i^2 \delta_i(t_1 - t_2) \text{ for } i = 1, 2.$$

The intensity or strength of γ_i is denoted by $\mu_i > 0$ in this case. The Dirac delta function δ_i is defined as follows:

$$\begin{cases} \delta_i(x) = 0, \text{ for } x \neq 0, \\ \int_{-\infty}^{\infty} \delta_i(x) dx = 1 \end{cases}$$

where $\langle \cdot \rangle$ is the ensemble average of the stochastic process under consideration. So, system (6) is modified as follows :

$$\begin{aligned} \frac{dx_1}{dt} &= \alpha x_1 \left(\frac{1 + \beta x_1}{1 + \beta x_1 + \delta x_2} \right) - (m_1 + \gamma_1(t))x_1 - d_1 x_1^2 - \frac{d_2 x_1 x_2}{\rho + \xi \mu A + x_1} - v_1 x_1^3, \\ \frac{dx_2}{dt} &= \frac{cd_2(x_1 + \mu A)x_2}{\rho + \xi \mu A + x_1} - (m_2 + \gamma_2(t))x_2 - v_2 x_2^2, \\ \implies \frac{dx_1}{dt} &= \alpha x_1 \left(\frac{1 + \beta x_1}{1 + \beta x_1 + \delta x_2} \right) - m_1 x_1 - d_1 x_1^2 - \frac{d_2 x_1 x_2}{\rho + \xi \mu A + x_1} - v_1 x_1^3 - \sigma_1 x_1 \frac{dw_1}{dt}, \\ \frac{dx_2}{dt} &= \frac{cd_2(x_1 + \mu A)x_2}{\rho + \xi \mu A + x_1} - m_2 x_2 - v_2 x_2^2 - \sigma_2 x_2 \frac{dw_2}{dt}. \end{aligned} \tag{30}$$

Here, we take $\gamma_1 = \sigma_1 \frac{dw_1}{dt}$ and $\gamma_2 = \sigma_2 \frac{dw_2}{dt}$, where $w = \{w_1(t), w_2(t) \mid t \geq 0\}$ denotes standard Brownian motion in two-dimension. It is assumed that $m_i + \gamma_i(t)$ is positive and bounded for $i = 1, 2$.

Thus, from (30), we have the following stochastic system:

$$\begin{aligned} dx_1 &= \left[\alpha x_1 \left(\frac{1 + \beta x_1}{1 + \beta x_1 + \delta x_2} \right) - m_1 x_1 - d_1 x_1^2 - \frac{d_2 x_1 x_2}{\rho + \xi \mu A + x_1} - v_1 x_1^3 \right] dt - \sigma_1 x_1 dw_1, \\ dx_2 &= \left[\frac{cd_2(x_1 + \mu A)x_2}{\rho + \xi \mu A + x_1} - m_2 x_2 - v_2 x_2^2 \right] dt - \sigma_2 x_2 dw_2. \end{aligned} \tag{31}$$

We have already defined parameters in Table 1. The Euler Maruyama method is used in MATLAB to determine the dynamical behavior of system (31). We have studied the system behavior numerically and depicted the results in Figures 9, 10 and 11, with $\sigma_1 = 0.009$ and $\sigma_2 = 0.002$.

Figure 9 illustrates the impact of environmental fluctuations on the stability of coexistence steady states. In Figure 9a, we present the time series of prey and predator populations in both stochastic and deterministic systems. The trajectories of prey populations are denoted by (◊), (—), while the trajectories of predator populations are represented by (◊), (—) in stochastic and deterministic systems, respectively. This depiction reveals that due to environmental fluctuations, the trajectories closely align with the deterministic trajectory's values, which reflects a realistic scenario. It would seem implausible for population sizes to remain constant over time, indicating an absence of external factors affecting the system. In addition to the time series presented in Figure 9a, the corresponding histograms are depicted in Figure 9b. These histograms illustrate the frequency distributions of the population sizes for both prey and predator populations.

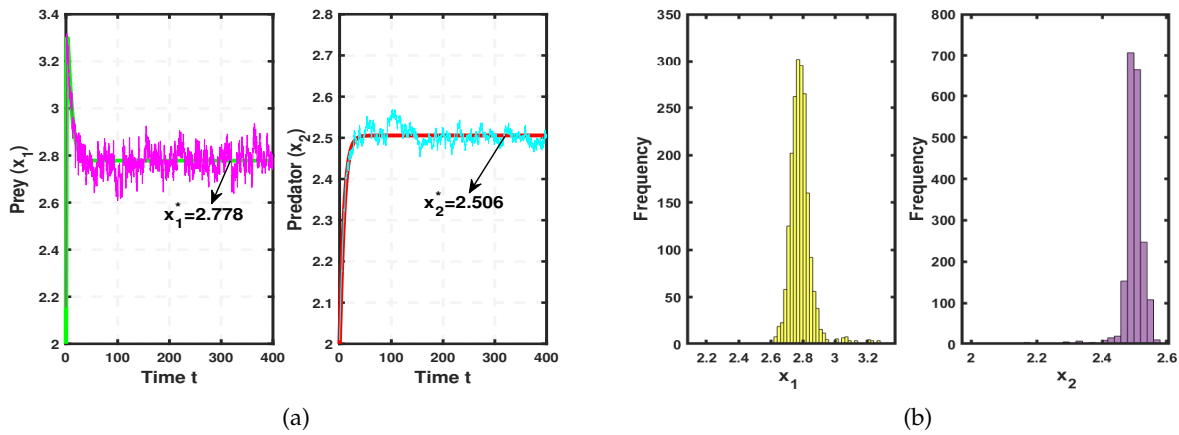


Figure 9: **(a)** Trajectories of the species in deterministic model (6) and stochastic model (31). Here, (◊), (—) indicate the trajectories of prey population and (◊), (—) indicate the trajectories of predator population in stochastic and deterministic system, respectively. **(b)** Histograms of the species corresponding to the system (30). All the parameters values are given in Table 2.

Figure 10 illustrates the temporal evolution and population distribution of species in both stochastic and deterministic systems corresponding to the predator-free steady state E_{a_1} . In the Figure 10a, (◊) and (—) denote the trajectories of the prey population, while (◊) and (—) represent the trajectories of the predator population in the stochastic and deterministic systems, respectively. It's worth noting that the trajectories of the stochastic system exhibit fluctuations around those of the deterministic system, as observed in previous cases. Additionally, Figure 10b provides histograms to visually represent the distribution of populations, offering further insight into the dynamics of the system.

Similarly to the aforementioned cases, we also observe the impact of environmental fluctuations on the prey-free steady state E_{a_2} , as depicted in Figure 11. This observation yields results similar to those previously discussed.

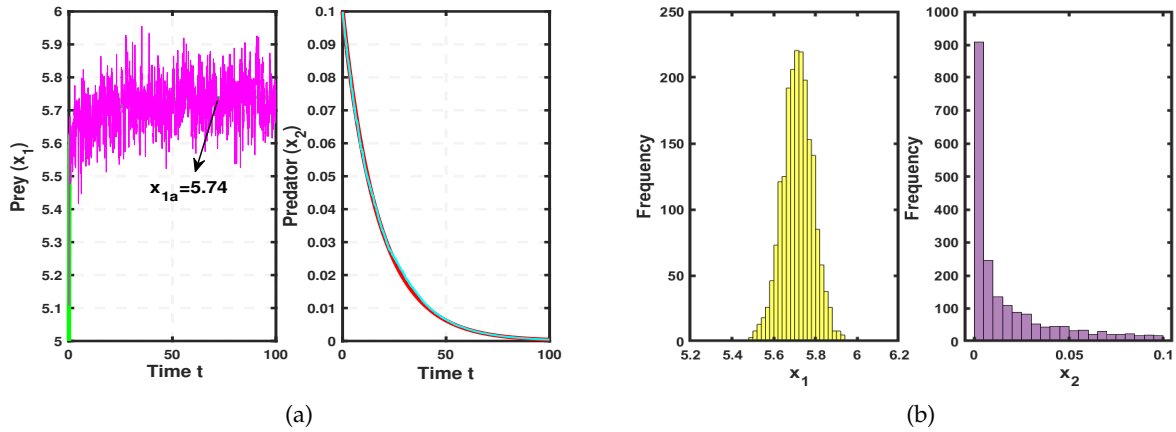


Figure 10: **(a)** Trajectories of the species in deterministic model (6) and stochastic model (31). Here, (—), (—) indicate the trajectories of prey population and (—), (—) indicate the trajectories of predator population in stochastic and deterministic system, respectively. **(b)** Histograms of the species corresponding to the system (30). Here, $m_2 = 0.25$ and other parameters values are given in Table 2.

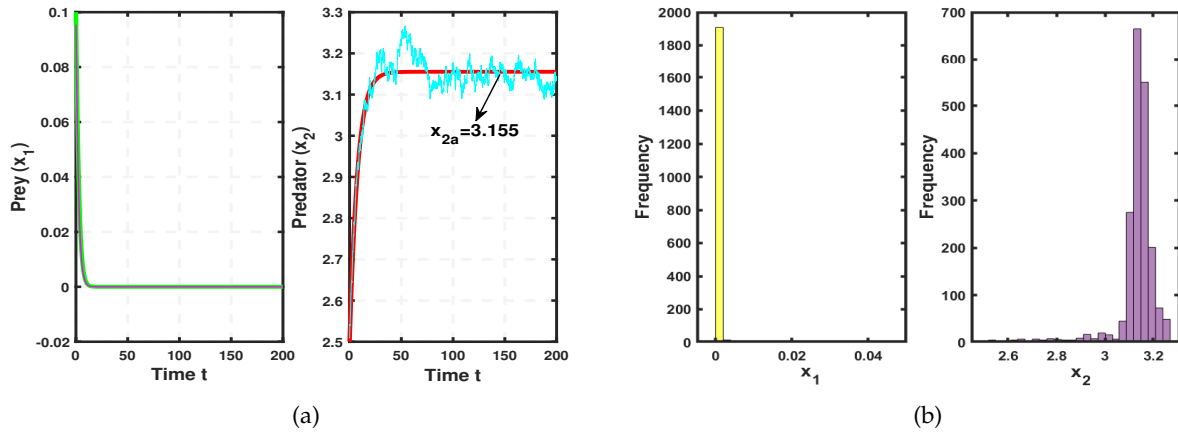


Figure 11: **(a)** Trajectories of the species in deterministic model (6) and stochastic model (31). Here, (—), (—) indicate the trajectories of prey population and (—), (—) indicate the trajectories of predator population in stochastic and deterministic system, respectively. **(b)** Histograms of the species corresponding to the system (30). Here, $m_2 = 0.02$ and other parameters values are given in Table 2.

8. Discussions

The interplay between predators and prey species within ecological systems is multifaceted, encompassing both direct and indirect impacts. While direct impacts involve physical encounters leading to predation, indirect impacts, often non-lethal, can significantly shape ecosystem dynamics. Research suggests that indirect impacts, such as fear induced by the presence of predators, can be even more influential in altering prey behaviors and population dynamics. Fear-induced changes can affect prey populations by reducing reproductive success rates, altering grazing behavior, and even driving evolutionary changes over time. Again, understanding the concept of carryover effects is important in elucidating the complex dynamics between predators and prey. Carryover effects highlight the long-term consequences of past interactions on individual prey and entire populations. This concept is particularly relevant in evolutionary biology

and ecology, where scientists aim to unravel the intricate relationships between several-species within an ecosystem. Incorporating time delays into predator-prey models further enhances their ability to capture real-life dynamics. The presence of toxic materials in the environment poses significant risks to both humans and predator-prey species. The type, concentration, duration of exposure, and biological/ecological characteristics of the organisms involved all play crucial roles in determining the extent of the impact. Time delays account for the lag between actions and their consequences, encompassing factors such as gestation and maturation time, population response time, migration, environmental fluctuations, and evolutionary changes. By integrating time delays, mathematical models can offer a more accurate portrayal of temporal dynamics, thereby deepening our understanding of how populations respond to environmental changes over time. Moreover, environmental stochasticity introduces additional complexity to ecological models by accounting for fluctuations in population birth and mortality rates driven by factors like temperature, humidity, parasites, pollutants, and food availability. While deterministic models may overlook these fluctuations, stochastic approaches, particularly those incorporating Gaussian white noise, offer a more realistic representation of rapidly changing environmental conditions. Recognizing the significance of the factors outlined above, we delve into our predator-prey model, incorporating fear-induced responses, additional food supply for predator and carry-over effects within a toxic environment. Additionally, we also incorporate time delays, treating them as gestation delays. Furthermore, we investigate the influence of environmental fluctuations by examining the stochastic system corresponding to our model. In our analysis we get the following insight:

The bifurcation diagrams depicted in Figures 1, 2, 3, and 4 offer comprehensive insights into the system's dynamic behavior concerning various parameters such as A , δ , m_1 , m_2 , v_1 , v_2 , and β .

In Figure 1, we observe critical points indicating significant transitions in system behavior. Notably, at $A_{[BP]} = 2.216$, unstable branches emerge for E_0 and E_{a_2} , marking a branch point. Subsequently, transcritical and saddle node bifurcations occur at $A_{[TC]} = 4.407$ and $A_{[SN]} = 7.365$, respectively. The highlighted region illustrates bistability between interior equilibrium points E_c and prey-free equilibrium E_{a_2} . Similarly, Figure 1b displays transcritical and saddle node bifurcations at $\delta_{[TC]} = 2.986$ and $\delta_{[SN]} = 7.029$, respectively.

Figure 2 provides insights into bifurcation scenarios concerning parameters m_1 and m_2 , revealing transcritical and saddle node bifurcations at $m_{1[TC]} = 0.2018$, $m_{2[TC]} = 0.1047$, and $m_{1[SN]} = 0.7348$, $m_{2[SN]} = 0.0417$, respectively.

In Figures 3 and 4, we explore the bifurcation phenomena related to v_1 , v_2 , and β , as well as in the m_1m_2 and v_1v_2 -planes. These diagrams elucidate the emergence of saddle node bifurcations, transcritical bifurcations, and regions of bistability, delineating stability patterns across parameter spaces.

Moreover, the phase portrait and nullcline illustrated in Figure 5 provide a visual representation of the system's dynamic behavior, emphasizing the presence of stable nodes, unstable nodes, and saddle points across varying initial conditions. This holistic analysis enhances our understanding of the system's intricate dynamics within the defined parameter space, offering valuable insights into its stability and behavior.

The bifurcation diagram depicted in Figure 6 for the delayed system (10) highlights the occurrence of Hopf bifurcation at the critical point $\tau^* = 13.96$. This critical point signifies a transition in the stability characteristics of the system. For delay parameter values τ less than τ^* , the system remains stable, while for values exceeding τ^* , instability arises. To illustrate this phenomenon, we conducted a comparative analysis for two distinct values of τ : $\tau = 9 < \tau^*$ and $\tau = 16 > \tau^*$. Figure 7 showcases the stable behavior of the system for $\tau = 9$, with trajectories converging towards a stable equilibrium point. Conversely, Figure 8 demonstrates oscillatory behavior for $\tau = 16$, with trajectories forming a stable limit cycle. This analysis underscores the critical role of the delay parameter τ in determining the stability and dynamic behavior of the system.

Using the Euler-Maruyama method implemented in MATLAB, we have investigated the behavior of system (31) under environmental stochasticity, employing $\sigma_1 = 0.009$ and $\sigma_2 = 0.002$ as parameter values. Our numerical exploration have been culminated due to the depiction of results in Figures 9, 10, and 11.

Figure 9 provides insights into how environmental fluctuations influence the stability of coexistence steady states. Specifically, in Figure 9a, we have presented time series data for prey and predator populations, comparing stochastic and deterministic systems. Trajectories of prey and predator populations in stochastic systems are represented by distinct symbols and lines, showcasing fluctuations driven by

environmental noise. Remarkably, these trajectories closely align with deterministic trajectories, indicating realistic deviations from constant population sizes over time. Moreover, Figure 9b complements the time series data by presenting histograms illustrating the frequency distributions of population sizes for both prey and predator populations. These histograms offer additional insights into the variability induced by environmental stochasticity, providing a comprehensive understanding of population dynamics under fluctuating environmental conditions.

Although the suggested model reveals some interesting dynamics, there are several phenomena that we may incorporate into the model in order to increase its realism with the surrounding environment. Further exploration of the model can be carried out by incorporating a ratio-dependent functional response for interactions between healthy prey and predators. In addition to this, a diffusive model can be explored by implementing spatio-temporal effects to investigate the spatial pattern.

Acknowledgement

The first author (Bijoy Kumar Das) is thankful to the Council of Scientific & Industrial Research, India for providing SRF.

Data Availability Statement

The data that has been utilized to support the outcomes of this investigation is contained in the article.

Conflict of Interest

The authors declare that they have no conflict of interest regarding this work.

Appendix A

$$A_1 = \beta v_1^2 v_2$$

$$A_2 = \beta d_1 v_1 v_2 + c \delta d_2 v_1 v_2 - \delta m_2 v_1 v_2 + v_1^2 v_2 + 3A\beta \mu \xi v_1^2 v_2 + 3\beta \rho v_1^2 v_2$$

$$A_3 = - \left(- c \delta d_1 d_2 v_2 + \delta d_1 m_2 v_2 + \alpha \beta v_1 v_2 - d_1 v_1 v_2 - 3A\beta \mu \xi d_1 v_1 v_2 - 3\beta \rho d_1 v_1 v_2 - A c \delta \mu d_2 v_1 v_2 - 2A c \delta \mu \xi d_2 v_1 v_2 - 2c \delta \rho d_2 v_1 v_2 - \beta m_1 v_1 v_2 + 3A \delta \mu \xi m_2 v_1 v_2 + 3 \delta \rho m_2 v_1 v_2 - 3A \mu \xi v_1^2 v_2 - 3A^2 \beta \mu^2 \xi^2 v_1^2 v_2 - 3 \rho v_1^2 v_2 - 6A \beta \mu \xi \rho v_1^2 v_2 - 3 \beta \rho^2 v_1^2 v_2 \right)$$

$$A_4 = - \left(- c \beta d_2^2 v_1 + \beta d_2 m_2 v_1 - A c \delta \mu d_1 d_2 v_2 - 2A c \delta \mu \xi d_1 d_2 v_2 - 2c \delta \rho d_1 d_2 v_2 - c \delta d_2 m_1 v_2 + 3A \delta \mu \xi d_1 m_2 v_2 + 3 \delta \rho d_1 m_2 v_2 + \delta m_1 m_2 v_2 + \alpha v_1 v_2 + 3A \alpha \beta \mu \xi v_1 v_2 + 3 \alpha \beta \rho v_1 v_2 - 3A \mu \xi d_1 v_1 v_2 - 3A^2 \beta \mu^2 \xi^2 d_1 v_1 v_2 - 3 \rho d_1 v_1 v_2 - 6A \beta \mu \xi \rho d_1 v_1 v_2 - 3 \beta \rho^2 d_1 v_1 v_2 - 2A^2 c \delta \mu^2 \xi d_2 v_1 v_2 - A^2 c \delta \mu^2 \xi^2 d_2 v_1 v_2 - 2A c \delta \mu \rho d_2 v_1 v_2 - 2A c \delta \mu \xi \rho d_2 v_1 v_2 - c \delta \rho^2 d_2 v_1 v_2 - m_1 v_1 v_2 - 3A \beta \mu \xi m_1 v_1 v_2 - 3 \beta \rho m_1 v_1 v_2 + 3A^2 \delta \mu^2 \xi^2 m_2 v_1 v_2 + 6A \delta \mu \xi \rho m_2 v_1 v_2 + 3 \delta \rho^2 m_2 v_1 v_2 - 3A^2 \mu^2 \xi^2 v_1^2 v_2 - A^3 \beta \mu^3 \xi^3 v_1^2 v_2 - 6A \mu \xi \rho v_1^2 v_2 - 3A^2 \beta \mu^2 \xi^2 \rho v_1^2 v_2 - 3 \rho^2 v_1^2 v_2 - 3A \beta \mu \xi \rho^2 v_1^2 v_2 - \beta \rho^3 v_1^2 v_2 \right)$$

$$A_5 = - \left(- c^2 \delta d_2^3 + 2c \delta d_2^2 m_2 - \delta d_2 m_2^2 - c d_2^2 v_1 - A c \beta \mu d_2^2 v_1 - A c \beta \mu \xi d_2^2 v_1 - c \beta \rho d_2^2 v_1 + d_2 m_2 v_1 + 2A \beta \mu \xi d_2 m_2 v_1 + 2 \beta \rho d_2 m_2 v_1 - 2A^2 c \delta \mu^2 \xi d_1 d_2 v_2 - A^2 c \delta \mu^2 \xi^2 d_1 d_2 v_2 - 2A c \delta \mu \rho d_1 d_2 v_2 - 2A c \delta \mu \xi \rho d_1 d_2 v_2 - c \delta \rho^2 d_1 d_2 v_2 - A c \delta \mu d_2 m_1 v_2 - 2A c \delta \mu \xi d_2 m_1 v_2 - 2c \delta \rho d_2 m_1 v_2 + 3A^2 \delta \mu^2 \xi^2 d_1 m_2 v_2 + 6A \delta \mu \xi \rho d_1 m_2 v_2 + 3 \delta \rho^2 d_1 m_2 v_2 + 3A \delta \mu \xi m_1 m_2 v_2 + 3 \delta \rho m_1 m_2 v_2 + 3A \alpha \mu \xi v_1 v_2 + 3A^2 \alpha \beta \mu^2 \xi^2 v_1 v_2 + 3 \alpha \rho v_1 v_2 \right)$$

$$\begin{aligned}
& + 6A\alpha\beta\mu\xi\rho v_1 v_2 + 3\alpha\beta\rho^2 v_1 v_2 - 3A^2\mu^2\xi^2 d_1 v_1 v_2 - A^3\beta\mu^3\xi^3 d_1 v_1 v_2 - 6A\mu\xi\rho d_1 v_1 v_2 - 3A^2\beta\mu^2\xi^2 \rho d_1 v_1 v_2 \\
& - 3\rho^2 d_1 v_1 v_2 - 3A\beta\mu\xi\rho^2 d_1 v_1 v_2 - \beta\rho^3 d_1 v_1 v_2 - A^3 c\delta\mu^3\xi^2 d_2 v_1 v_2 - 2A^2 c\delta\mu^2\xi\rho d_2 v_1 v_2 - A c\delta\mu\rho^2 d_2 v_1 v_2 \\
& - 3A\mu\xi m_1 v_1 v_2 - 3A^2\beta\mu^2\xi^2 m_1 v_1 v_2 - 3\rho m_1 v_1 v_2 - 6A\beta\mu\xi\rho m_1 v_1 v_2 - 3\beta\rho^2 m_1 v_1 v_2 + A^3\delta\mu^3\xi^3 m_2 v_1 v_2 \\
& + 3A^2\delta\mu^2\xi^2 \rho m_2 v_1 v_2 + 3A\delta\mu\xi\rho^2 m_2 v_1 v_2 + \delta\rho^3 m_2 v_1 v_2 - A^3\mu^3\xi^3 v_1^2 v_2 - 3A^2\mu^2\xi^2 \rho v_1^2 v_2 - 3A\mu\xi\rho^2 v_1^2 v_2 \\
& - \rho^3 v_1^2 v_2)
\end{aligned}$$

$$\begin{aligned}
A_6 = & - \left(- 2Ac^2\delta\mu d_2^3 + 2Ac\delta\mu d_2^2 m_2 + 2Ac\delta\mu\xi d_2^2 m_2 + 2c\delta\rho d_2^2 m_2 - 2A\delta\mu\xi d_2 m_2^2 - 2\delta\rho d_2 m_2^2 - A c\mu d_2^2 v_1 \right. \\
& - A c\mu\xi d_2^2 v_1 - A^2 c\beta\mu^2\xi d_2^2 v_1 - c\rho d_2^2 v_1 - A c\beta\mu\rho d_2^2 v_1 + 2A\mu\xi d_2 m_2 v_1 + A^2\beta\mu^2\xi^2 d_2 m_2 v_1 + 2\rho d_2 m_2 v_1 \\
& + 2A\beta\mu\xi\rho d_2 m_2 v_1 + \beta\rho^2 d_2 m_2 v_1 - A^3 c\delta\mu^3\xi^2 d_1 d_2 v_2 - 2A^2 c\delta\mu^2\xi\rho d_1 d_2 v_2 - A c\delta\mu\rho^2 d_1 d_2 v_2 - 2A^2 c\delta\mu^2\xi d_2 m_1 v_2 \\
& - A^2 c\delta\mu^2\xi^2 d_2 m_1 v_2 - 2Ac\delta\mu\rho d_2 m_1 v_2 - 2Ac\delta\mu\xi\rho d_2 m_1 v_2 - c\delta\rho^2 d_2 m_1 v_2 + A^3\delta\mu^3\xi^3 d_1 m_2 v_2 \\
& + 3A^2\delta\mu^2\xi^2 \rho d_1 m_2 v_2 + 3A\delta\mu\xi\rho^2 d_1 m_2 v_2 + \delta\rho^3 d_1 m_2 v_2 + 3A^2\delta\mu^2\xi^2 m_1 m_2 v_2 + 6A\delta\mu\xi\rho m_1 m_2 v_2 \\
& + 3\delta\rho^2 m_1 m_2 v_2 + 3A^2\alpha\mu^2\xi^2 v_1 v_2 + A^3\alpha\beta\mu^3\xi^3 v_1 v_2 + 6A\alpha\mu\xi\rho v_1 v_2 + 3A^2\alpha\beta\mu^2\xi^2 \rho v_1 v_2 + 3\alpha\rho^2 v_1 v_2 \\
& + 3A\alpha\beta\mu\xi\rho^2 v_1 v_2 + \alpha\beta\rho^3 v_1 v_2 - A^3\mu^3\xi^3 d_1 v_1 v_2 - 3A^2\mu^2\xi^2 \rho d_1 v_1 v_2 - 3A\mu\xi\rho^2 d_1 v_1 v_2 - \rho^3 d_1 v_1 v_2 \\
& - 3A^2\mu^2\xi^2 m_1 v_1 v_2 - A^3\beta\mu^3\xi^3 m_1 v_1 v_2 - 6A\mu\xi\rho m_1 v_1 v_2 - 3A^2\beta\mu^2\xi^2 \rho m_1 v_1 v_2 - 3\rho^2 m_1 v_1 v_2 \\
& \left. - 3A\beta\mu\xi\rho^2 m_1 v_1 v_2 - \beta\rho^3 m_1 v_1 v_2 \right)
\end{aligned}$$

$$\begin{aligned}
A_7 = & - \left(- A^2 c^2\delta\mu d_2^3 + 2A^2 c\delta\mu^2\xi d_2^2 m_2 + 2Ac\delta\mu\rho d_2^2 m_2 - A^2\delta\mu^2\xi^2 d_2 m_2^2 - 2A\delta\mu\xi\rho d_2 m_2^2 - \delta\rho^2 d_2 m_2^2 \right. \\
& - A^2 c\mu^2\xi d_2^2 v_1 - A c\mu\rho d_2^2 v_1 + A^2\mu^2\xi^2 d_2 m_2 v_1 + 2A\mu\xi\rho d_2 m_2 v_1 + \rho^2 d_2 m_2 v_1 - A^3 c\delta\mu^3\xi^2 d_2 m_1 v_2 \\
& - 2A^2 c\delta\mu^2\xi\rho d_2 m_1 v_2 - A c\delta\mu\rho^2 d_2 m_1 v_2 + A^3\delta\mu^3\xi^3 m_1 m_2 v_2 + 3A^2\delta\mu^2\xi^2 \rho m_1 m_2 v_2 + 3A\delta\mu\xi\rho^2 m_1 m_2 v_2 \\
& + \delta\rho^3 m_1 m_2 v_2 + A^3\alpha\mu^3\xi^3 v_1 v_2 + 3A^2\alpha\mu^2\xi^2 \rho v_1 v_2 + 3A\alpha\mu\xi\rho^2 v_1 v_2 + \alpha\rho^3 v_1 v_2 - A^3\mu^3\xi^3 m_1 v_1 v_2 \\
& \left. - 3A^2\mu^2\xi^2 \rho m_1 v_1 v_2 - 3A\mu\xi\rho^2 m_1 v_1 v_2 - \rho^3 m_1 v_1 v_2 \right)
\end{aligned}$$

References

- [1] T. R. Malthus, *An Essay on the Principle of Population as It Affects the Future Improvement of Society, with Remarks on the Speculations of Mr. Godwin, M. Condorcet, and Other Writers*, The Lawbook Exchange Ltd., 1986.
- [2] P. F. Verhulst, *Notice sur la loi que la population suit dans son accroissement*, *Corresp. Math. Phys* **10(2)** (1838), 113-126. <https://doi.org/10.1016/j.mbs.2012.11.007>
- [3] A. J. Lotka, *Elements of physical biology*, Williams and Wilkins company (1925).
- [4] V. Volterra, *Variazioni e fluttuazioni del numero d'individui in specie animali conviventi*, *Memoria della Reale Accademia Nazionale dei Lincei* (1927).
- [5] S. L. Lima, *Nonlethal Effects in the Ecology of Predator-Prey Interactions*, *BioScience* **48(1)** (1998), 25-34. <https://doi.org/10.2307/1313225>
- [6] S. Creel, D. Christianson, S. Liley, J. A. Winnie, *Predation Risk Affects Reproductive Physiology and Demography of Elk*, *Science* **315(5814)** (2007), 960. <https://doi.org/10.1126/science.1135918>
- [7] W. Cresswell, *Predation in bird populations*, *J Ornithol* **152** (2011), 251–263.
- [8] A. Duro, V. Piccione, M. A. Ragusa, V. Veneziano, *New environmentally sensitive patch index-ESPI-for MEDALUIS protocol*, *American Institute of Physics* **1637** (2014), 305–312.
- [9] V. Piccione, M. A. Ragusa, V. Rapicavoli, V. Veneziano, *Monitoring of a natural park through ESPI*, *AIP Publishing LLC* **1978** (2018), 140005.
- [10] S. Saha, G. P. Samanta, *Analysis of a tritrophic food chain model with fear effect incorporating prey refuge*, *Filomat* **35(15)** (2021), 4971–4999.
- [11] R. P. Agarwal, O. Bazighifan, M. A. Ragusa, *Nonlinear neutral delay differential equations of fourth-order: oscillation of solutions*, *Entropy* **23(2)** (2021), 129.
- [12] C.S. Holling, *Some Characteristics of Simple Types of Predation and Parasitism*, *The Canadian Entomologist* **91(07)** (1959), 385–398. <https://doi.org/10.4039/ent91385-7>
- [13] M. J. Sheriff, C. J. Krebs, R. Boonstra, *The sensitive hare: sublethal effects of predator stress on reproduction in snowshoe hares*, *Journal of Animal Ecology* **78(6)** (2009), 1249-1258. <https://doi.org/10.1111/j.1365-2656.2009.01552.x>
- [14] L. Y. Zanette, A. F. White, M. C. Allen, M. Clinchy, *Perceived Predation Risk Reduces the Number of Offspring Songbirds Produce per Year*, *Science* **334(6061)** (2011), 1398-1401. <https://doi.org/10.1126/science.1210908>
- [15] D. Sahoo, G. P. Samanta, *Impact of Fear Effect in a Two Prey-One Predator System with Switching Behaviour in Predation*, *Differential Equations and Dynamical Systems* **32** (2024), 377-399. <https://doi.org/10.1007/s12591-021-00575-7>

- [16] B. K. Das, D. Sahoo, G. P. Samanta, *Impact of fear in a delay-induced predator–prey system with intraspecific competition within predator species*, *Mathematics and Computers in Simulation* **191** (2022), 134–156. <https://doi.org/10.1016/j.matcom.2021.08.005>
- [17] O. J. Schmitz, A. P. Beckerman, K. M. O'Brien, *Behaviorally mediated trophic cascades: Effects of predation risk on food web interactions*, *Ecological Society of America* **78(5)** (1997), 1388–1399. [https://doi.org/10.1890/0012-9658\(1997\)078\[1388:BMTCEO\]2.0.CO;2](https://doi.org/10.1890/0012-9658(1997)078[1388:BMTCEO]2.0.CO;2)
- [18] B. K. Das, D. Sahoo, N. Santra, G. Samanta, *Modeling predator–prey interaction: effects of perceived fear and toxicity on ecological communities*, *Int. J. Dynam. Control* (2023). <https://doi.org/10.1007/s40435-023-01343-x>
- [19] C. M. O'Connor, D. R. Norris, G. T. Crossin, S. J. Cooke, *Biological carryover effects: linking common concepts and mechanisms in ecology and evolution*, *Ecosphere* **5(3)** (2014), 1–11. <https://doi.org/10.1890/ES13-00388.1>
- [20] S. Mondal, G. P. Samanta, *A comparison study of predator–prey system in deterministic and stochastic environments influenced by fear and its carry-over effects*, *The European Physical Journal Plus* **137(70)** (2022). <https://doi.org/10.1140/epjp/s13360-021-02219-9>
- [21] B. K. Das, D. Sahoo, G. Samanta, *Fear and its carry-over effects in a delay-induced predator–prey model with additional food to predator*, *Filomat* **37(18)** (2023), 6059–6088. <https://doi.org/10.2298/FIL2318059D>
- [22] T. K. Kar, K. S. Chaudhuri, *On non-selective harvesting of two competing fish species in the presence of toxicity*, *Ecological Modelling* **161** (2003), 125–137. [https://doi.org/10.1016/s0304-3800\(02\)00323-x](https://doi.org/10.1016/s0304-3800(02)00323-x)
- [23] T. Das, R. N. Mukherjee, K. S. Chaudhuri, *Harvesting of a prey–predator fishery in the presence of toxicity*, *Applied Mathematical Modelling* **33(5)** (2009), 2282–2292. <https://doi.org/10.1016/j.apm.2008.06.008>
- [24] A. Das, G. P. Samanta, *Modelling the fear effect in a two-species predator–prey system under the influence of toxic substances*, *Rendiconti del Circolo Matematico di Palermo Series 2* **70** (2021), 1501–1526. <https://doi.org/10.1007/s12215-020-00570-x>
- [25] P. Dutta, D. Sahoo, S. Mondal, G. P. Samanta, *Dynamical complexity of a delay-induced eco-epidemic model with Beddington DeAngelis incidence rate*, *Mathematics and Computers in Simulation* **197** (2022), 45–90. <https://doi.org/10.1016/j.matcom.2022.02.002>
- [26] N. Santra, S. Saha, G. Samanta, *Role of multiple time delays on a stage-structured predator–prey system in a toxic environment*, *Mathematics and Computers in Simulation* **212** (2023), 548–583. <https://doi.org/10.1016/j.matcom.2023.05.015>
- [27] N. Santra, D. Sahoo, S. Mondal, G. Samanta, *An epidemiological multi-delay model on cassava mosaic disease with delay-dependent parameters*, *Filomat* **37(9)** (2023), 2887–2921. <https://doi.org/10.2298/FIL2309887S>
- [28] N. Santra, S. Mondal, G. Samanta, *Complex Dynamics of a Predator–Prey Interaction with Fear Effect in Deterministic and Fluctuating Environments*, *Mathematics* **10(20)** (2022), 3795. <https://doi.org/10.3390/math10203795>
- [29] A. Das, G.P. Samanta, *A prey–predator model with refuge for prey and additional food for predator in a fluctuating environment*, *Physica A: Statistical Mechanics and its Applications* **538** (2019), 427–450. <https://doi.org/10.1016/j.physa.2019.122844>
- [30] A. Das, G. P. Samanta, *Modeling the fear effect on a stochastic prey–predator system with additional food for the predator*, *Journal of Physics A: Mathematical and Theoretical* **51** (2018), 465601(26pp). <https://doi.org/10.1088/1751-8121/aae4c6>
- [31] J. K. Hale, *Retarded functional differential equations: basic theory*, *Theory of functional differential equations* (1977), 36–56.
- [32] L. Perko, *Differential Equations and Dynamical Systems*, Vol. 7 (Springer Science & Business Media), 2013.
- [33] S. Ruan, J. Wei, *On the zeros of transcendental functions with applications to stability of delay differential equations with two delays*, *Dynamics of Continuous, Discrete and Impulsive Systems Series B: Applications and Algorithms* **10** (2003), 863–874.